

---

# Uniform Kernel Prober

---

000  
001  
002  
003  
004  
005  
006  
007  
008  
009  
010  
011  
012  
013  
014  
015  
016  
017  
018  
019  
020  
021  
022  
023  
024  
025  
026  
027  
028  
029  
030  
031  
032  
033  
034  
035  
036  
037  
038  
039  
040  
041  
042  
043  
044  
045  
046  
047  
048  
049  
050  
051  
052  
053  
054

Anonymous Authors<sup>1</sup>

## Abstract

The ability to identify useful features or representations of the input data based on training data that achieves low prediction error on test data across multiple prediction tasks is considered the key to multitask learning success. In practice, however, one faces the issue of the choice of prediction tasks and the availability of test data from the chosen tasks while comparing the relative performance of different features. In this work, we develop a class of pseudometrics called Uniform Kernel Prober (UKP) for comparing features or representations learned by different statistical models such as neural networks when the downstream prediction tasks involve kernel ridge regression. The proposed pseudometric, UKP, between any two representations, provides a uniform measure of prediction error on test data corresponding to a general class of kernel ridge regression tasks for a given choice of a kernel without access to test data. Additionally, desired invariances in representations can be successfully captured by UKP only through the choice of the kernel function and the pseudometric can be efficiently estimated from  $n$  input data samples with  $O(\frac{1}{\sqrt{n}})$  estimation error. We also experimentally demonstrate the ability of UKP to discriminate between different types of features or representations based on their generalization performance on downstream kernel ridge regression tasks.

## 1. Introduction

Model comparison is a classical problem in Statistics and Machine Learning (Burnham et al., 1998; Pfahringer et al., 2000; Spiegelhalter et al., 2002; Caruana & Niculescu-Mizil, 2006; Fernández-Delgado et al., 2014). This question has received tremendous attention from the scientific community,

especially after the widespread adoption and implementation of modern general-purpose large-scale models such as deep neural networks (DNNs). Faced with the vast complexity and variation in mathematical representations (functional forms), sizes (no. of trainable parameters), and levels of model transparency (open to public vs. black-box/query access), it is an ongoing challenge to develop criteria for model comparison that is general and widely applicable to a large class of models as well as choice of learning tasks.

In the supervised learning setting, where the goal is to predict the correct outputs given some inputs, it is natural to compare models based on relative differences in predictive performance, as this aligns directly with the objective of maximizing model accuracy on the supervised learning task. It is now well understood that the key to success for training models with good generalization ability over multiple tasks (i.e. achieves low prediction error on test data across multiple prediction tasks) is directly correlated to the ability of models to identify useful features or representations of the input data based on training data (Bengio et al., 2013; LeCun et al., 2015; Maurer et al., 2016). Therefore, one can attempt to resolve the question of model comparison by considering metrics (more precisely, pseudometrics) on the space of features or representations, and there is extensive literature in this area (Laakso & Cottrell, 2000; Li et al., 2015; Morcos et al., 2018; Wang et al., 2018; Kornblith et al., 2019; Boix-Adsera et al., 2022).

An ideal pseudometric must be interpretable and efficiently computable based on a reasonably small amount of data samples. It must also be sensitive only to differences in features that will lead to differences in predictive performance, but be fairly insensitive to any other differences in features that do not affect predictive performance. Finally, it must be flexible enough to accommodate available prior knowledge about the class of prediction tasks that is of interest to the model users. However, most pseudometrics fall short of fulfilling this extensive set of desiderata. In this work, we develop a class of pseudometrics on the space of representations called Uniform Kernel Prober (UKP) that can be used to compare features or representations learned by any class of statistical models.

The proposed pseudometric is motivated by the need for a distance measure over representations of differing dimensionalities that captures the ability of a model to generalize

<sup>1</sup>Anonymous Institution, Anonymous City, Anonymous Region, Anonymous Country. Correspondence to: Anonymous Author <anon.email@domain.com>.

Preliminary work. Under review by the International Conference on Machine Learning (ICML). Do not distribute.

over a general and flexible class of prediction tasks, specifically, the class of kernel ridge regression-based tasks. Depending on the choice of the kernel, one can probe which models share “similar” features, with similarity being understood in the following sense: If the features or representations for a pair of models are similar, then, if they are both trained to perform kernel ridge regression tasks, their predictive performances will be close to each other.

The proposed UKP pseudometric is a unique distance measure over features or representations and is a useful contribution to the existing literature since it has the following desirable characteristics:

1. The proposed pseudometric offers a uniform guarantee of performance similarity for a wide range of regression functions, irrespective of whether the tasks are kernel ridge-regression or not. This is particularly beneficial when the prediction tasks align with models whose representations share similar characteristics with the kernel used to compute the UKP distance.

2. The pseudometric is adaptable to incorporate inductive biases that help identify models suited for specific tasks. A simple choice of the kernel parameter of the UKP distance can help us encode these inductive biases. For example, suppose we are interested in image classification tasks where the rotation of the images should not affect the model prediction. In that case, we can encode this inductive bias into the pseudometric by choosing a rotationally invariant kernel, such as a Gaussian RBF kernel, as the kernel parameter for UKP. This results in the creation of two clusters: one for models with rotationally invariant features and another for models without such features.

To the best of our knowledge, ours is the first pseudometric on the space of representations in the ML literature that can flexibly encode a wide range of inductive biases and treat them within a single framework.

3. UKP distance has a practical prediction-based interpretation in addition to usual mathematical interpretations of similarity or dissimilarity in terms of inner product or pseudometric.

4. Computation of the estimate of UKP distance only requires unlabelled data, i.e., data samples from the input domain, and therefore preserves labeled data for model training/fitting. Moreover, the computation of the estimate of UKP distance only requires black-box access to model representations, i.e., pairs of inputs and outputs to the model.

5. It is possible to design a statistically efficient estimator for the UKP distance based on a finite number ( $n$ ) of

samples from the input domain, that enjoys an estimation error rate of  $n^{-1/2}$ .

6. The UKP distance enables us to even compare representations that differ in their dimensionalities.

The paper is organized as follows. In Section 2, we formally define the UKP distance. In Section 3, we provide different characterizations of the UKP distance and prove that it satisfies all criteria of being a pseudometric. Then using Lemma 2, we also find the type of transformations under which the UKP distance remains invariant. We propose a statistical estimator of the UKP distance in Section 4. In Sections 4.1 and 4.2, we mathematically demonstrate its relationship to other pseudometrics used for model comparison and show that our proposed estimator converges to the true UKP distance as the sample size goes to infinity. Finally, in Section 5, we provide numerical experiments that validate our theory. Proofs of all lemmas, propositions and theorems are provided in Section A.1 of the Appendix.

## 2. Problem setup

Let the input/predictor of the model be  $X \in \mathbb{R}^d$  and  $P_X$  be the distribution of the input. Let  $\phi : \mathbb{R}^d \rightarrow \mathbb{R}^k$  and  $\psi : \mathbb{R}^d \rightarrow \mathbb{R}^l$  be two instances of a representation map that transforms an input to a feature representation used in a trained/fitted model. Let  $Y$  be the random real-valued response corresponding to the input  $X$  generated from the nonparametric regression model  $Y = \eta(X) + \epsilon$  where  $\epsilon$  is mean-zero noise, where  $\eta(x) = \mathbb{E}(Y | X = x)$  is the population regression function of  $Y$  on  $X$ .

Let  $K(\cdot, \cdot)$  be a positive definite, symmetric, bounded, and continuous kernel function, mapping pairs of vectors in Euclidean spaces of different dimensions to real numbers. Examples of radial kernels include the Gaussian RBF kernel  $K_{RBF,h}(x, y) = \exp(-\frac{1}{2h} \|x - y\|_2^2)$  and the Laplace kernel  $K_{Lap,h}(x, y) = \exp(-\frac{1}{2h} \|x - y\|_1)$ , where  $x, y \in \mathbb{R}^d$  for any  $d \in \mathbb{N}$ . By the Moore-Aronszajn Theorem (Aronszajn, 1950) and Lemma 4.33 of Steinwart & Christmann (2008), there exists a unique separable Reproducing Kernel Hilbert Space (RKHS)  $\mathcal{H}$  of functions such that  $K(\cdot, \cdot)$  is its unique reproducing kernel. Theorem 5.7 of Paulsen & Raghupathi (2016) ensures that  $K_\phi(\cdot, \cdot) := K(\phi(\cdot), \phi(\cdot))$  and  $K_\psi(\cdot, \cdot) := K(\psi(\cdot), \psi(\cdot))$  are the unique reproducing kernels corresponding to the “pullback” RKHS’s  $\mathcal{H}_\phi := \mathcal{H}(K \circ (\phi \times \phi))$  and  $\mathcal{H}_\psi := \mathcal{H}(K \circ (\psi \times \psi))$ . Further, let  $\mathcal{H}^k$  and  $\mathcal{H}^l$  be the RKHS’s associated with the kernel  $K$  when the domain is restricted to  $\mathbb{R}^k \times \mathbb{R}^k$  and  $\mathbb{R}^l \times \mathbb{R}^l$ , respectively. Then, for any  $f_\phi \in \mathcal{H}_\phi$ , we have  $\|f_\phi\|_{\mathcal{H}_\phi} = \min_{f \in \mathcal{H}^k: f \circ \phi = f_\phi} \|f\|_{\mathcal{H}^k}$  and for any  $f_\psi \in \mathcal{H}_\psi$ , we have  $\|f_\psi\|_{\mathcal{H}_\psi} = \min_{f \in \mathcal{H}^l: f \circ \psi = f_\psi} \|f\|_{\mathcal{H}^l}$ .

For any  $\lambda > 0$ , let  $\alpha_\lambda$  and  $\beta_\lambda$  be the population kernel ridge regression estimators of the regression function  $\eta$ , given by

$$\alpha_\lambda = \arg \min_{\alpha \in \mathcal{H}_\phi} \mathbb{E} [Y - \alpha(X)]^2 + \lambda \|\alpha\|_{\mathcal{H}_\phi}^2 \quad (1)$$

and

$$\beta_\lambda = \arg \min_{\beta \in \mathcal{H}_\psi} \mathbb{E} [Y - \beta(X)]^2 + \lambda \|\beta\|_{\mathcal{H}_\psi}^2, \quad (2)$$

respectively. The prediction loss being the squared error loss,  $\alpha_\lambda$  and  $\beta_\lambda$  depend on the distribution of  $Y$  only through the population regression function  $\eta$ .

We now define the kernel ridge regression-based pseudometric between the two representations of the input  $\phi$  and  $\psi$ , based on the difference between predictions for  $Y$  uniformly over all regression functions  $\eta \in L^2(P_X)$  such that its  $L^2(P_X)$  norm is bounded above by 1.

**Definition 1.** For any  $\lambda > 0$  and choice of kernel  $K(\cdot, \cdot)$ , the UKP (Uniform Kernel Prober) distance between representations  $\phi(X)$  and  $\psi(X)$  is defined as,

$$d_{\lambda, K}^{\text{UKP}}(\phi, \psi) := \sup_{\|\eta\|_{L^2(P_X)} \leq 1} \left( \mathbb{E} [\alpha_\lambda(X) - \beta_\lambda(X)]^2 \right)^{\frac{1}{2}},$$

where  $\alpha_\lambda$  and  $\beta_\lambda$  are defined in Equations (1) and (2), respectively.

### 3. Properties of $d_{\lambda, K}^{\text{UKP}}$

Let  $\mathcal{I}_\phi : \mathcal{H}_\phi \rightarrow L^2(P_X)$ ,  $f \rightarrow f$  be the inclusion operator, which maps any  $f \in \mathcal{H}_\phi$  to its representation  $f \in L^2(P_X)$ . Then the adjoint of the inclusion operator is given by  $\mathcal{I}_\phi^* : L^2(P_X) \rightarrow \mathcal{H}_\phi$ ,  $f \rightarrow \int K_\phi(\cdot, x)f(x)dP_X(x)$ . The inclusion operator  $\mathcal{I}_\psi$  and the corresponding adjoint operator  $\mathcal{I}_\psi^*$  can be analogously defined.

Let us define the covariance operators corresponding to the RKHS's  $\mathcal{H}_\phi$  and  $\mathcal{H}_\psi$  as follows:

$$\begin{aligned} \Sigma_\phi &:= \int K_\phi(\cdot, x) \otimes_{\mathcal{H}_\phi} K_\phi(\cdot, x)dP_X(x) \\ &= \int K(\phi(\cdot), \phi(x)) \otimes_{\mathcal{H}_\phi} K(\phi(\cdot), \phi(x))dP_X(x) \end{aligned}$$

and

$$\begin{aligned} \Sigma_\psi &:= \int K_\psi(\cdot, x) \otimes_{\mathcal{H}_\psi} K_\psi(\cdot, x)dP_X(x) \\ &= \int K(\psi(\cdot), \psi(x)) \otimes_{\mathcal{H}_\psi} K(\psi(\cdot), \psi(x))dP_X(x). \end{aligned}$$

$\Sigma_\phi : \mathcal{H}_\phi \rightarrow \mathcal{H}_\phi$  and  $\Sigma_\psi : \mathcal{H}_\psi \rightarrow \mathcal{H}_\psi$  are the unique operators that satisfy

$$\langle \Sigma_\phi f_1, g_1 \rangle_{\mathcal{H}_\phi} = \mathbb{E} [f_1(X)g_1(X)]$$

and

$$\langle \Sigma_\psi f_2, g_2 \rangle_{\mathcal{H}_\psi} = \mathbb{E} [f_2(X)g_2(X)],$$

where  $f_1, g_1 \in \mathcal{H}_\phi$  and  $f_2, g_2 \in \mathcal{H}_\psi$ , respectively. In terms of inclusion operators, it can be easily shown that  $\Sigma_\phi = \mathcal{I}_\phi^* \mathcal{I}_\phi$  and  $\Sigma_\psi = \mathcal{I}_\psi^* \mathcal{I}_\psi$ .

Let us define the integral operators corresponding to the RKHS's  $\mathcal{H}_\phi$  and  $\mathcal{H}_\psi$  as follows:

$$\mathcal{T}_\phi f := \int K_\phi(\cdot, x)f(x)dP_X(x)$$

and

$$\mathcal{T}_\psi f := \int K_\psi(\cdot, x)f(x)dP_X(x),$$

for any  $f \in L^2(P_X)$ . It is also easy to show that  $\mathcal{T}_\phi = \mathcal{I}_\phi \mathcal{I}_\phi^*$  and  $\mathcal{T}_\psi = \mathcal{I}_\psi \mathcal{I}_\psi^*$ . The boundedness and continuity of the kernel  $K$  ensures that  $\Sigma_\phi$ ,  $\Sigma_\psi$ ,  $\mathcal{T}_\phi$  and  $\mathcal{T}_\psi$  are all compact trace-class operators, which consequently ensures that they are also Hilbert-Schmidt operators. Further, each of  $\Sigma_\phi$ ,  $\Sigma_\psi$ ,  $\mathcal{T}_\phi$  and  $\mathcal{T}_\psi$  are self-adjoint positive operators and therefore have a spectral representation (Reed & Simon, 1980, Theorems VI.16, VI.17).

For any  $\lambda > 0$ , the regularized inverse covariance operators are defined as  $\Sigma_\phi^{-\lambda} := (\Sigma_\phi + \lambda I)^{-1}$  and  $\Sigma_\psi^{-\lambda} := (\Sigma_\psi + \lambda I)^{-1}$ , while the corresponding square roots are defined as  $\Sigma_\phi^{-\frac{\lambda}{2}} := (\Sigma_\phi + \lambda I)^{-\frac{1}{2}}$  and  $\Sigma_\psi^{-\frac{\lambda}{2}} := (\Sigma_\psi + \lambda I)^{-\frac{1}{2}}$ . Further, let us define  $\tilde{K}_\phi(x, y) := \Sigma_\phi^{-\frac{\lambda}{2}} K_\phi(x, y)$  and  $\tilde{K}_\psi(x, y) := \Sigma_\psi^{-\frac{\lambda}{2}} K_\psi(x, y)$ .

The UKP distance has the following characterization:

**Lemma 1.** For any  $\lambda > 0$ , the squared UKP distance  $d_{\lambda, K}^{\text{UKP}}(\phi, \psi)$  between representations  $\phi(X)$  and  $\psi(X)$  can be expressed as

$$\begin{aligned} &[d_{\lambda, K}^{\text{UKP}}(\phi, \psi)]^2 \\ &= \mathbb{E} \left[ \left\langle \Sigma_\phi^{-\frac{\lambda}{2}} K_\phi(\cdot, X), \Sigma_\phi^{-\frac{\lambda}{2}} K_\phi(\cdot, X') \right\rangle_{\mathcal{H}_\phi} \right. \\ &\quad \left. - \left\langle \Sigma_\psi^{-\frac{\lambda}{2}} K_\psi(\cdot, X), \Sigma_\psi^{-\frac{\lambda}{2}} K_\psi(\cdot, X') \right\rangle_{\mathcal{H}_\psi} \right]^2 \\ &= \mathbb{E} \left[ \left\langle K_\phi(\cdot, X), \Sigma_\phi^{-\lambda} K_\phi(\cdot, X') \right\rangle_{\mathcal{H}_\phi} \right. \\ &\quad \left. - \left\langle K_\psi(\cdot, X), \Sigma_\psi^{-\lambda} K_\psi(\cdot, X') \right\rangle_{\mathcal{H}_\psi} \right]^2, \end{aligned}$$

where  $X$  and  $X'$  are i.i.d observations drawn from  $P_X$ .

The proof is provided in Section A.1.1 of the Appendix. The above characterization shows that the UKP induces an isometric embedding  $\phi \mapsto \left\langle \Sigma_\phi^{-\frac{\lambda}{2}} K_\phi(\cdot, X), \Sigma_\phi^{-\frac{\lambda}{2}} K_\phi(\cdot, X') \right\rangle_{\mathcal{H}_\phi}$  of  $\phi$  into

165  $L^2(P_X^{\otimes 2})$ . This characterization allows us to prove  
 166 Proposition 1, which will be useful throughout the rest of  
 167 the paper.

168 Next, we show that the UKP distance can be expressed  
 169 in terms of the trace operator, which will be essential for  
 170 developing a statistical estimator of the pseudometric based  
 171 on random samples from the input distribution  $P_X$ .

172 To do so, we define the cross-covariance operators  $\Sigma_{\phi\psi} : \mathcal{H}_\psi \rightarrow \mathcal{H}_\phi$  and  $\Sigma_{\psi\phi} : \mathcal{H}_\phi \rightarrow \mathcal{H}_\psi$  as follows:

$$176 \quad \Sigma_{\phi\psi} := \int K_\phi(\cdot, x) \otimes_{\mathcal{L}^2(\mathcal{H}_\psi, \mathcal{H}_\phi)} K_\psi(\cdot, x) dP_X(x) \\ 177 \\ 178 = \int K(\phi(\cdot), \phi(x)) \otimes_{\mathcal{L}^2(\mathcal{H}_\psi, \mathcal{H}_\phi)} K(\psi(\cdot), \psi(x)) dP_X(x)$$

180 and

$$183 \quad \Sigma_{\psi\phi} := \int K_\psi(\cdot, x) \otimes_{\mathcal{L}^2(\mathcal{H}_\phi, \mathcal{H}_\psi)} K_\phi(\cdot, x) dP_X(x) \\ 184 \\ 185 = \int K(\psi(\cdot), \psi(x)) \otimes_{\mathcal{L}^2(\mathcal{H}_\phi, \mathcal{H}_\psi)} K(\phi(\cdot), \phi(x)) dP_X(x) \\ 186 \\ 187 = \Sigma_{\phi\psi}^*. \\ 188$$

189 **Proposition 1.** For any  $\lambda > 0$ , the squared UKP distance  
 190  $d_{\lambda,K}^{\text{UKP}}(\phi, \psi)$  between representations  $\phi(X)$  and  $\psi(X)$  can  
 191 be expressed as

$$193 \quad [d_{\lambda,K}^{\text{UKP}}(\phi, \psi)]^2 \\ 194 \\ 195 = \text{Tr} \left( \Sigma_\phi^{-\lambda} \Sigma_\phi \Sigma_\phi^{-\lambda} \Sigma_\phi \right) + \text{Tr} \left( \Sigma_\psi^{-\lambda} \Sigma_\psi \Sigma_\psi^{-\lambda} \Sigma_\psi \right) \\ 196 \\ 197 - 2 \text{Tr} \left( \Sigma_\phi^{-\lambda} \Sigma_{\phi\psi} \Sigma_\psi^{-\lambda} \Sigma_{\psi\phi} \right).$$

198 The proof is provided in Section A.1.2 of the Appendix.

200 The following theorem serves to show that the UKP distance  
 201 does satisfy the axioms of a pseudometric.

203 **Theorem 1.** For any  $\lambda > 0$ , the  $d_{\lambda,K}^{\text{UKP}}$  distance satisfies the  
 204 following properties:

- 206 1. For any function  $\phi : \mathbb{R}^d \rightarrow \mathbb{R}^k$  for some  $k \in \mathbb{N}$ ,  
 $d_{\lambda,K}^{\text{UKP}}(\phi, \phi) = 0$ ,
- 207 2. (Non-negativity) For any two functions  $\phi : \mathbb{R}^d \rightarrow \mathbb{R}^k$   
 208 and  $\psi : \mathbb{R}^d \rightarrow \mathbb{R}^l$  for some  $k, l \in \mathbb{N}$ ,  $d_{\lambda,K}^{\text{UKP}}(\phi, \psi) \geq 0$ ,
- 210 3. (Symmetric) For any two functions  $\phi : \mathbb{R}^d \rightarrow \mathbb{R}^k$   
 211 and  $\psi : \mathbb{R}^d \rightarrow \mathbb{R}^l$  for some  $k, l \in \mathbb{N}$ ,  $d_{\lambda,K}^{\text{UKP}}(\phi, \psi) =$   
 $d_{\lambda,K}^{\text{UKP}}(\psi, \phi)$ ,
- 213 4. (Triangle inequality) For any three functions  $\phi : \mathbb{R}^d \rightarrow$   
 214  $\mathbb{R}^k$ ,  $\psi : \mathbb{R}^d \rightarrow \mathbb{R}^l$  and  $\varphi : \mathbb{R}^d \rightarrow \mathbb{R}^m$  for some  
 215  $k, l, m \in \mathbb{N}$ ,  $d_{\lambda,K}^{\text{UKP}}(\phi, \psi) \leq d_{\lambda,K}^{\text{UKP}}(\phi, \varphi) + d_{\lambda,K}^{\text{UKP}}(\varphi, \psi)$ .

Hence,  $d_{\lambda,K}^{\text{UKP}}$  is a pseudometric over the space of all functions that maps  $\mathbb{R}^d$  to some Euclidean space  $\mathbb{R}^t$  for any  $t \in \mathbb{N}$ .

The proof is provided in Section A.1.3 of the Appendix.

We now analyze the invariance properties of the pseudometric  $d_{\lambda,K}^{\text{UKP}}$  and identify the transformations of the representations  $\phi$  and  $\psi$  that leave its value unchanged. To this end, the following lemma will be useful, whose proof is provided in Section A.1.4 of the Appendix.

**Lemma 2.** Let  $f : \mathbb{R}^d \rightarrow \mathbb{R}^k$  and  $g : \mathbb{R}^d \rightarrow \mathbb{R}^l$  be any two functions. Consider a positive definite, symmetric, bounded and continuous kernel function  $K(\cdot, \cdot)$  defined on the domain  $\cup_d \{\mathcal{X}_d \times \mathcal{X}_d\}$ , where  $\mathcal{X}_d \subset \mathbb{R}^d$  is a separable space for  $d \in \mathbb{N}$ . Let  $K_f(\cdot, \cdot) := K(f(\cdot), f(\cdot))$  and  $K_g(\cdot, \cdot) := K(g(\cdot), g(\cdot))$  be the unique reproducing kernels corresponding to the “pullback” RKHS’s  $\mathcal{H}_f := \mathcal{H}(K \circ (f \times f))$  and  $\mathcal{H}_g := \mathcal{H}(K \circ (g \times g))$ . For any  $\lambda > 0$ , let  $\Sigma_f^{-\frac{\lambda}{2}}$  and  $\Sigma_g^{-\frac{\lambda}{2}}$  denote the square roots of the  $\lambda$ -regularized covariance operators corresponding to the kernels  $K_f$  and  $K_g$ , respectively. For any  $x, x' \in \mathbb{R}^d$  and  $\lambda > 0$ , define the operator  $\mathcal{I}$  as follows:

$$\mathcal{I}(f)(x, x') = \left\langle \Sigma_f^{-\frac{\lambda}{2}} K_f(\cdot, x), \Sigma_f^{-\frac{\lambda}{2}} K_f(\cdot, x') \right\rangle_{\mathcal{H}_f} \\ = \left\langle K_f(\cdot, x), \Sigma_f^{-\lambda} K_f(\cdot, x') \right\rangle_{\mathcal{H}_f}.$$

Then, a necessary and sufficient condition for  $f$  and  $g$  to satisfy  $\mathcal{I}(f) = \mathcal{I}(g)$  is that  $K_f(\cdot, \cdot) = K_g(\cdot, \cdot)$ .

As an easy corollary of Lemma 2, we can identify representations that UKP treats as equivalent in terms of prediction-based performance for a general collection of kernel ridge regression tasks corresponding to a particular kernel  $K$ .

**Corollary 1.** Let  $\mathcal{H}$  be the class of transformations under which the kernel  $K$  is invariant, i.e.,  $\mathcal{H} = \{h : K(\cdot, \cdot) = K(h(\cdot), h(\cdot)) \text{ a.e. } P_X\}$ . Then, the UKP distance  $d_{\lambda,K}^{\text{UKP}}(\phi, \psi)$  between representations  $\phi(X)$  and  $\psi(X)$  is invariant under the same class of transformations that the kernel  $K$  is invariant for, i.e., for any  $h_1, h_2 \in \mathcal{H}$ ,

$$d_{\lambda,K}^{\text{UKP}}(h_1 \circ \phi, h_2 \circ \psi) = d_{\lambda,K}^{\text{UKP}}(\phi, \psi)$$

and if either  $h_1$  or  $h_2$  does not belong to  $\mathcal{H}$ ,

$$d_{\lambda,K}^{\text{UKP}}(h_1 \circ \phi, h_2 \circ \psi) \neq d_{\lambda,K}^{\text{UKP}}(\phi, \psi).$$

The proof of Corollary 1 is provided in Section A.1.5 of the Appendix.

Based on these results, the following corollary of Lemma 2 then provides an exact characterization of the representations that lead to  $d_{\lambda,K}^{\text{UKP}} = 0$ .

**Corollary 2.** A necessary and sufficient condition for the UKP distance  $d_{\lambda,K}^{\text{UKP}}(\phi, \psi)$  between representations  $\phi(X)$  and  $\psi(X)$  to be zero is that  $K_\phi(\cdot, \cdot) = K_\psi(\cdot, \cdot)$  a.e.  $P_X$ .

The proof is straightforward, similar to that of Corollary 1, and is therefore omitted.

## 4. Statistical estimation of $d_{\lambda,K}^{\text{UKP}}$

In practice, when comparing the prediction-based utility of different representations, we consider the realistic scenario where one only has access to a random sample  $X_1, \dots, X_n \stackrel{i.i.d.}{\sim} P_X$  and a statistical estimator of the proposed distance measure is required. In supervised learning settings, the goal is to allocate most of the data for training and model fitting while minimizing the amount of data used for diagnostics and exploratory analysis.

Using the empirical covariance and cross-covariance operators  $\hat{\Sigma}_\phi$ ,  $\hat{\Sigma}_\psi$ ,  $\hat{\Sigma}_{\phi\psi}$  and  $\hat{\Sigma}_{\psi\phi} = \hat{\Sigma}_{\phi\psi}^*$  as plug-in estimators of  $\Sigma_\phi$ ,  $\Sigma_\psi$ ,  $\Sigma_{\phi\psi}$  and  $\Sigma_{\psi\phi}$  in the trace operator based expression of  $d_{\lambda,K}^{\text{UKP}}(\phi, \psi)$  as derived in Proposition 1, we arrive at the following V-statistic type estimator of  $d_{\lambda,K}^{\text{UKP}}(\phi, \psi)$ :

$$\begin{aligned} & \hat{d}_{\lambda,K}^{\text{UKP}}(\phi, \psi) \\ &= \left[ \text{Tr} \left( \hat{\Sigma}_\phi^{-\lambda} \hat{\Sigma}_\phi \hat{\Sigma}_\phi^{-\lambda} \hat{\Sigma}_\phi \right) + \text{Tr} \left( \hat{\Sigma}_\psi^{-\lambda} \hat{\Sigma}_\psi \hat{\Sigma}_\psi^{-\lambda} \hat{\Sigma}_\psi \right) \right. \\ &\quad \left. - 2 \text{Tr} \left( \hat{\Sigma}_\phi^{-\lambda} \hat{\Sigma}_{\phi\psi} \hat{\Sigma}_\psi^{-\lambda} \hat{\Sigma}_{\psi\phi} \right) \right]^{\frac{1}{2}}, \end{aligned} \quad (3)$$

where

$$\begin{aligned} \hat{\Sigma}_\phi &= \frac{1}{n} \sum_{i=1}^n K_\phi(\cdot, X_i) \otimes_{\mathcal{H}_\phi} K_\phi(\cdot, X_i) \\ &= \frac{1}{n} \sum_{i=1}^n K(\phi(\cdot), \phi(X_i)) \otimes_{\mathcal{H}_\phi} K(\phi(\cdot), \phi(X_i)), \end{aligned}$$

$$\begin{aligned} \hat{\Sigma}_\psi &= \frac{1}{n} \sum_{i=1}^n K_\psi(\cdot, X_i) \otimes_{\mathcal{H}_\psi} K_\psi(\cdot, X_i) \\ &= \frac{1}{n} \sum_{i=1}^n K(\psi(\cdot), \psi(X_i)) \otimes_{\mathcal{H}_\psi} K(\psi(\cdot), \psi(X_i)), \end{aligned}$$

$$\begin{aligned} \hat{\Sigma}_{\phi\psi} &= \frac{1}{n} \sum_{i=1}^n K_\phi(\cdot, X_i) \otimes_{\mathcal{L}^2(\mathcal{H}_\psi, \mathcal{H}_\phi)} K_\psi(\cdot, X_i) \\ &= \frac{1}{n} \sum_{i=1}^n K(\phi(\cdot), \phi(X_i)) \otimes_{\mathcal{L}^2(\mathcal{H}_\psi, \mathcal{H}_\phi)} K(\psi(\cdot), \psi(X_i)), \end{aligned}$$

and

$$\begin{aligned} \hat{\Sigma}_{\psi\phi} &= \frac{1}{n} \sum_{i=1}^n K_\psi(\cdot, X_i) \otimes_{\mathcal{L}^2(\mathcal{H}_\phi, \mathcal{H}_\psi)} K_\phi(\cdot, X_i) \\ &= \frac{1}{n} \sum_{i=1}^n K(\psi(\cdot), \psi(X_i)) \otimes_{\mathcal{L}^2(\mathcal{H}_\phi, \mathcal{H}_\psi)} K(\phi(\cdot), \phi(X_i)) \\ &= \hat{\Sigma}_{\phi\psi}^*. \end{aligned}$$

It is an easy exercise to show that the V-statistic type estimator  $\hat{d}_{\lambda,K}^{\text{UKP}}(\phi, \psi)$  can be expressed in terms of the number of input data points  $n$ , the chosen regularization parameter  $\lambda$  and the empirical Gram matrices  $K_{n,\phi}$  and  $K_{n,\psi}$  whose  $(i,j)$ -th elements are the kernel evaluations for the  $(i,j)$ -th input data pair  $(X_i, X_j)$ , i.e.,  $(K_{n,\phi})_{ij} = K(\phi(X_i), \phi(X_j))$  and  $(K_{n,\psi})_{ij} = K(\psi(X_i), \psi(X_j))$ . If  $\lambda = 0$ , one is required to ensure the invertibility of  $K_{n,\phi}$  and  $K_{n,\psi}$ .

**Proposition 2.** For any  $\lambda > 0$ , the V-statistic type estimator  $\hat{d}_{\lambda,K}^{\text{UKP}}(\phi, \psi)$  of  $d_{\lambda,K}^{\text{UKP}}(\phi, \psi)$  between representations  $\phi(X)$  and  $\psi(X)$  can be expressed as

$$\begin{aligned} & \hat{d}_{\lambda,K}^{\text{UKP}}(\phi, \psi) \\ &= [\text{Tr} (K_{n,\phi}(K_{n,\phi} + n\lambda I)^{-1} K_{n,\phi}(K_{n,\phi} + n\lambda I)^{-1}) \\ &\quad + \text{Tr} (K_{n,\psi}(K_{n,\psi} + n\lambda I)^{-1} K_{n,\psi}(K_{n,\psi} + n\lambda I)^{-1}) \\ &\quad - 2 \text{Tr} (K_{n,\phi}(K_{n,\phi} + n\lambda I)^{-1} K_{n,\psi}(K_{n,\psi} + n\lambda I)^{-1})]^\frac{1}{2}. \end{aligned}$$

### 4.1. Relation to other comparison measures

In this subsection, we discuss the relationship between the UKP distance and some popular distances between representations that are popularly used in Machine Learning.

The UKP distance is a generalization of the GULP distance, as proposed in Boix-Adsera et al. (2022), in the sense that, if we choose the kernel for the UKP to be the linear kernel  $K_{lin}(x, y) = x^T y$ , we exactly recover the GULP distance. Our proposed pseudometric  $\hat{d}_{\lambda,K}^{\text{UKP}}$  provides the additional flexibility of choosing other kernel functions, such as the Gaussian RBF kernel  $K_{RBF,h}$  and the Laplace  $K_{Lap,h}$ , for understanding the relative difference between the generalization performance on different classes of kernel ridge regression-based prediction tasks.

Let  $K_{n,\phi} = U_\phi \Lambda_{n,\phi} U_\phi^T$  and  $K_{n,\psi} = U_\psi \Lambda_{n,\psi} U_\psi^T$  be the eigenvalue decompositions of  $K_{n,\phi}$  and  $K_{n,\psi}$ , respectively. Here  $\Lambda_{n,\phi} = \text{diag} \left\{ \mu_\phi^{(1)}, \dots, \mu_\phi^{(n)} \right\}$  and  $\Lambda_{n,\psi} = \text{diag} \left\{ \mu_\psi^{(1)}, \dots, \mu_\psi^{(n)} \right\}$ . Define  $c_{\phi,\psi}^{(i),(j)} = (u_\phi^{(i)})^T u_\psi^{(j)}$ , as the inner product between the  $i$ -th eigenvector  $u_\phi^{(i)}$  corresponding to the  $i$ -th eigenvalue  $\mu_\phi^{(i)}$  of  $K_{n,\phi}$  and  $j$ -th eigenvector  $u_\psi^{(j)}$  corresponding to the  $j$ -th eigenvalue  $\mu_\psi^{(j)}$  of  $K_{n,\psi}$ . In the following proposition, we express the V-statistic type estimator  $\hat{d}_{\lambda,K}^{\text{UKP}}(\phi, \psi)$  exclusively in terms of the inner products  $c_{\phi,\psi}^{(i),(j)}$ ,  $s$ , the regularization parameter  $\lambda$  and the eigenvalues  $\mu_\phi^{(i)}$ 's and  $\mu_\psi^{(j)}$ 's, which is useful for understanding the effect of changing the regularization parameter  $\lambda$  on the estimate and its relation to other popular pseudometrics on the space of representations.

**Proposition 3.** For any  $\lambda > 0$ , the V-statistic type estimator  $\hat{d}_{\lambda,K}^{\text{UKP}}(\phi, \psi)$  of  $d_{\lambda,K}^{\text{UKP}}(\phi, \psi)$  between representations  $\phi(X)$

and  $\psi(X)$  can be expressed as

$$\begin{aligned} \hat{d}_{\lambda,K}^{\text{UKP}}(\phi, \psi) &= \left[ \sum_{i=1}^n \left( \frac{\mu_\phi^{(i)}}{\mu_\phi^{(i)} + n\lambda} \right)^2 + \sum_{j=1}^n \left( \frac{\mu_\psi^{(j)}}{\mu_\psi^{(j)} + n\lambda} \right)^2 \right. \\ &\quad \left. - 2 \sum_{i=1}^n \sum_{j=1}^n \frac{\mu_\phi^{(i)} \mu_\psi^{(j)}}{(\mu_\phi^{(i)} + n\lambda)(\mu_\psi^{(j)} + n\lambda)} \left( c_{\phi,\psi}^{(i),(j)} \right)^2 \right]^{\frac{1}{2}}. \end{aligned}$$

The proof is straightforward, relying on the spectral decomposition of  $K_{n,\phi}$  and  $K_{n,\psi}$  and the properties of the trace operator, and is thus omitted.

The general kernelized version of the Ridge-CCA (Canonical Correlation Analysis) distance, introduced by [Vinod \(1976\)](#) and later discussed in [M.Kuss & Graepel \(2003\)](#), is defined as

$$\begin{aligned} \hat{d}_{\lambda,K}^{\text{RCCA}}(\phi, \psi) &= \text{Tr} \left( \hat{\Sigma}_\phi^{-\lambda} \hat{\Sigma}_{\phi\psi} \hat{\Sigma}_\psi^{-\lambda} \hat{\Sigma}_{\psi\phi} \right) \\ &= \sum_{i=1}^n \sum_{j=1}^n \frac{\mu_\phi^{(i)} \mu_\psi^{(j)}}{(\mu_\phi^{(i)} + n\lambda)(\mu_\psi^{(j)} + n\lambda)} \left( c_{\phi,\psi}^{(i),(j)} \right)^2. \end{aligned}$$

However, the machine learning literature has largely focused on the original Ridge-CCA formulation with a linear kernel, as discussed in [Kornblith et al. \(2019\)](#). The classical CCA distance  $\hat{d}^{\text{CCA}}$  can be derived from the kernelized Ridge-CCA distance  $\hat{d}_{\lambda,K}^{\text{RCCA}}$  by selecting a linear kernel and setting  $\lambda = 0$ . From these definitions, it is clear that UKP is a distance measure on the Hilbert space of representations, while the kernelized Ridge-CCA serves as the corresponding inner product on the Hilbert space when the kernel and regularization parameter  $\lambda$  are the same for both.

Another related notion of distance, as proposed in [Cristianini et al. \(2001\)](#) and popularized by [Kornblith et al. \(2019\)](#), is known as CKA (Centered Kernel Alignment) and is defined as

$$\begin{aligned} \hat{d}_K^{\text{CKA}}(\phi, \psi) &= \frac{\text{Tr}(K_{n,\phi} H_n K_{n,\psi} H_n)}{\sqrt{\text{Tr}(K_{n,\phi} H_n K_{n,\phi} H_n) \text{Tr}(K_{n,\psi} H_n K_{n,\psi} H_n)}} \end{aligned}$$

where  $H_n = I_n - \frac{1}{n} \mathbf{1}_n \mathbf{1}_n^T$ . We can equivalently express  $\hat{d}_K^{\text{CKA}}(\phi, \psi)$  as

$$\begin{aligned} \hat{d}_K^{\text{CKA}}(\phi, \psi) &= \frac{\sum_{i=1}^n \sum_{j=1}^n \mu_\phi^{(i)} \mu_\psi^{(j)} \left( c_{\phi,\psi}^{(i),(j)} \right)^2}{\sqrt{\sum_{i=1}^n \left( \mu_\phi^{(i)} \right)^2} \sqrt{\sum_{j=1}^n \left( \mu_\psi^{(j)} \right)^2}}. \end{aligned}$$

If the kernelized Ridge-CCA distance is normalized by dividing it by the product of the norms of the pair of representations, taking the regularization parameter  $\lambda$  to  $+\infty$

recovers the CKA measure  $\hat{d}_K^{\text{CKA}}(\phi, \psi)$  in the limit. This can be shown by expressing  $\hat{d}_{\lambda,K}^{\text{UKP}}(\phi, \psi)$  and  $\hat{d}_K^{\text{CKA}}(\phi, \psi)$  in terms of the eigenvalues and eigenvectors of the empirical Gram matrices  $K_{n,\phi}$  and  $K_{n,\psi}$  and then taking the limit as  $\lambda \rightarrow +\infty$ . The kernelized Ridge-CCA distance thus serves as a bridge between the CKA measure, interpreted as a normalized inner product, and the UKP distance, understood as an unnormalized pseudometric in the space of representations. This connection implies a linear correlation between the two measures for sufficiently high value of the regularization parameter. While the CKA and kernelized Ridge-CCA measures naturally reflect similarity between representations via inner products, the UKP distance offers a broader perspective. Beyond functioning as a distance on the space of representations, it provides a relative measure of generalization performance uniformly across a wide range of prediction tasks involving kernel ridge regression—something other comparison measures fail to deliver.

It is desirable for discrepancy measures to satisfy pseudometric properties, particularly when comparing representations or features learned by DNN models. The UKP metric enables the assessment of similarity in generalization performance between two representations, even if they were not directly compared during experiments. This is especially useful when a sequence of proposed models is compared to a baseline but not to each other. For instance, suppose  $\phi_1$  represents a baseline model's representation. If one experimenter uses the UKP metric to compare  $\phi_1$  with a second representation  $\phi_2$ , while another experimenter compares  $\phi_1$  with a third representation  $\phi_3$ , the triangle inequality provides an upper bound for the UKP distance between  $\phi_2$  and  $\phi_3$ , even without directly comparing them. This eliminates the need for additional experiments, a valuable feature in the context of deep learning and large-scale data. In contrast, CKA cannot reuse such pairwise comparisons to approximate the similarity between  $\phi_2$  and  $\phi_3$ .

Most importantly, the UKP distance can differentiate between the generalization ability of models based on their associated representations/features without requiring any “training” on particular prediction-based tasks, which makes it efficient in terms of data and computational requirements.

## 4.2. Finite sample convergence rate of $\hat{d}_{\lambda,K}^{\text{UKP}}$

From a statistical estimation viewpoint, it is possible that the estimator  $\hat{d}_{\lambda,K}^{\text{UKP}}$  converges to  $d_{\lambda,K}^{\text{UKP}}$  as the number of data samples  $X_1, \dots, X_n$  from the input domain grows to infinity. In addition, we also provide a rate of convergence of the order of  $O(\frac{1}{\sqrt{n}})$ , which is a parametric rate of convergence. The following theorem, proved in Section A.1.6 of the Appendix, combines these two results and consequently illustrates the finite sample concentration of the estimator

330 proposed in Equation (3) around the population  $d_{\lambda,K}^{\text{UKP}}$ .  
 331

332 **Theorem 2.** Let  $\kappa$  be an upper bound on the kernel function  
 333  $K(\cdot, \cdot)$ . Then, for any  $\lambda > 0$  and  $\delta > 0$ , with probability  
 334 atleast  $1 - \delta$ , the V-statistic estimator  $\hat{d}_{\lambda}^{\text{UKP}}(\phi, \psi)$  satisfies

$$\begin{aligned} & \left| (d_{\lambda,K}^{\text{UKP}}(\phi, \psi))^2 - (\hat{d}_{\lambda}^{\text{UKP}}(\phi, \psi))^2 \right| \\ & \leq \frac{8\kappa^3}{\lambda^3} \left[ \frac{2\log(\frac{6}{\delta})}{n} + \sqrt{\frac{2\log(\frac{6}{\delta})}{n}} \right] \\ & \quad + \frac{4\kappa^2}{\lambda^2} \left[ \frac{2}{n} + \sqrt{\frac{2\log(\frac{6}{\delta})}{n}} \right]. \end{aligned}$$

### 345 4.3. Computational complexity of $\hat{d}_{\lambda,K}^{\text{UKP}}$

346 From the expression of the estimator  $\hat{d}_{\lambda,K}^{\text{UKP}}$  in Proposition  
 347 2, it can be shown that its computational complexity is  
 348  $O(n^3)$ , where  $n$  is the sample size. Notably, the GULP  
 349 distance proposed in Boix-Adsera et al. (2022) shares the  
 350 same complexity. The primary computational cost arises  
 351 from inverting the Gram matrix, which can be reduced using  
 352 kernel approximation techniques like Random Fourier  
 353 Features (RFF) or Nyström approximation. For example,  
 354 by using  $D$  RFF samples from the spectral distribution of  
 355 the kernel  $K$  or  $D$  subsamples from the  $n$  data samples  
 356 in the Nyström method, the complexity of the UKP  
 357 distance estimator  $\hat{d}_{\lambda,K}^{\text{UKP}}(\phi, \psi)$  can be reduced from  $O(n^3)$   
 358 to  $O(nD^2 + D^3)$ , which is significantly lower than  $O(n^3)$   
 359 when  $D \ll n$ . Exploring the tradeoff between the statistical  
 360 accuracy of UKP distance estimation and the computational  
 361 efficiency of kernel approximation methods is a promising  
 362 direction for future research.  
 363

## 364 5. Experiments

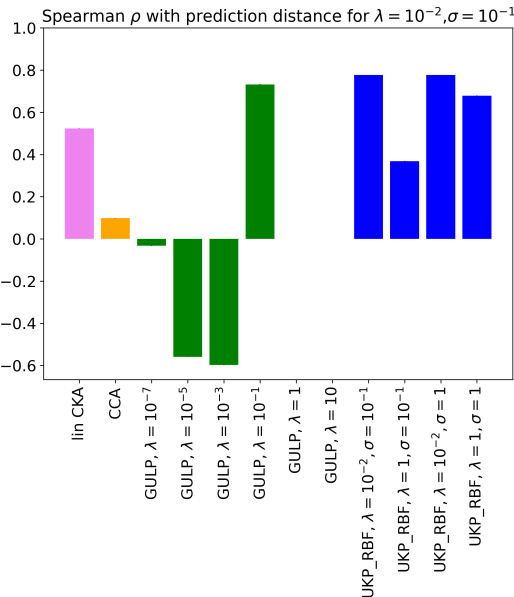
365 In this section, we present experimental results that show-  
 366 case the efficacy of the UKP distance in identifying simi-  
 367 larities and differences between representations relevant to  
 368 generalization performance on prediction tasks. Additional  
 369 experiments, including model architecture details and train-  
 370 ing, are provided in the Appendix. All computations were  
 371 performed on a single A100 GPU using Google Colab.  
 372

### 373 5.1. Ability of UKP to predict generalization 374 performance by kernel ridge regression-based 375 predictors

376 The UKP pseudometric gives a uniform bound on the dif-  
 377 ference in predictions generated by a pair of models, based  
 378 on kernel ridge regression-based estimators that utilize the  
 379 respective representations of the two models. It is a natural  
 380 question to ask if this uniform or worst-case guarantee on

381 the difference in prediction performance between represen-  
 382 tations is useful on a per-instance basis, i.e., given a specific  
 383 kernel ridge regression task, whether the UKP distance is  
 384 positively correlated with the generalization performance of  
 385 different models.

386 We consider 50 fully-connected neural networks with ReLU  
 387 activation, each having uniform widths of 200, 400, 700,  
 388 800, or 900 and depths ranging from 1 to 10. These networks  
 389 are trained on 60,000 28 × 28-pixel training images from  
 390 the MNIST handwritten digits dataset (Deng, 2012) for  
 391 50 epochs. Representations are then extracted from the  
 392 penultimate (final hidden) layer of each network, and the  
 393 CCA, linear CKA (CKA with a linear kernel), GULP, and  
 394 UKP distances are estimated for each pair of representations  
 395 using 5,000 test images from the same dataset.



396 Figure 1: Generalization of kernel ridge regression-based  
 397 predictors is strongly positively correlated with UKP  
 398 distance values. We report the average correlation across 10  
 399 random synthetic kernel ridge regression tasks. Error bars  
 400 are negligibly small and hence not visible.

401 We create synthetic kernel ridge regression tasks where  
 402 we randomly sample 5000 images and randomly assign a  
 403 standard Gaussian label to each image to create the synthetic  
 404 label/target vector. We obtain the kernel ridge regression  
 405 estimator for each representation with ridge penalty  $\lambda \in \{10^{-2}, 1\}$  and Gaussian RBF kernel with bandwidth  $\sigma \in \{10^{-1}, 1\}$ . The empirical mean of the squared difference  
 406 between predictions based on a pair of representations (say  $\phi$   
 407 and  $\psi$ ) is then computed using 5000 test images to estimate  
 408  $err_{\phi,\psi} = \mathbb{E}_{X \sim P_X} [\alpha_{\lambda}^{\phi}(X) - \alpha_{\lambda}^{\psi}(X)]^2$ , where  $\alpha_{\lambda}^{\phi}$  and  $\alpha_{\lambda}^{\psi}$   
 409 are the kernel ridge regression based predictors.

In Fig. 1, we plot the Spearman’s  $\rho$  rank correlation coefficient between the  $err_{\phi,\psi}$ ’s and the pairwise distances between the representations using CCA, linear CKA, GULP and UKP distances. For this particular regression task, we chose the synthetic ridge penalty to be  $\lambda = 10^{-2}$  and used a Gaussian RBF kernel with  $\sigma = 10^{-1}$ . For the UKP distance, we use the Gaussian RBF kernel as the choice of kernel.

We observe that the pairwise UKP distance is highly positively correlated with the collection of  $err_{\phi,\psi}$ ’s, as evident from the large positive values of the blue bars, with the largest correlation being observed when the ridge penalty used in the UKP distance matches with the synthetic ridge penalty we chose, i.e.,  $\lambda = 10^{-2}$ . In contrast, GULP distances exhibit inconsistent behavior across varying levels of regularization, while CCA and linear CKA distances show a significantly weaker positive correlation with generalization performance. As expected, due to the relationship between CKA and UKP discussed in Section 4.1, the CKA distance with a Gaussian RBF kernel performs comparably to UKP. Experiments with the remaining combinations of tuning parameters  $\lambda$  and  $\sigma$  are presented in Fig. 5 in Section A.2.1 of the Appendix, yielding qualitatively similar conclusions.

## 5.2. Ability of UKP to identify differences in architectures and inductive biases

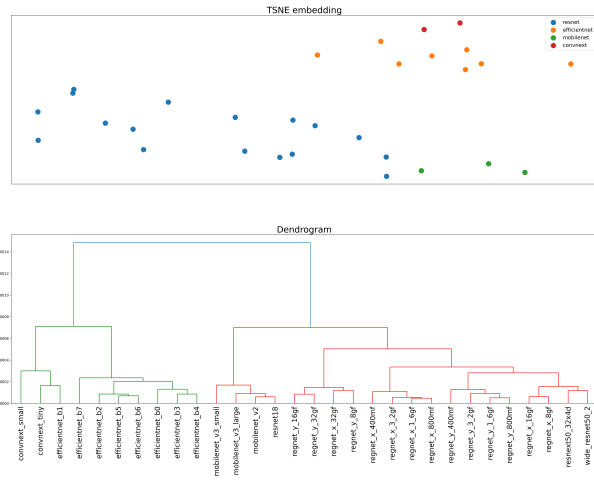


Figure 2: Clustering based on UKP distance is sensitive to differences in architectures of neural network models.

A key source of inductive biases in neural network models is their architecture, with features such as residual connections and variations in convolutional filter complexity shaping the representations learned during training. As a pseudometric over feature space, the UKP distance is expected to capture intrinsic differences in these inductive biases, which are known to impact generalization performance across tasks. To explore this, we analyze representations from 35 pre-

trained neural network architectures used for image classification, described in detail in Section A.2.2 of the Appendix.

We estimate pairwise UKP distances between model representations using 3,000 images from the validation set of the ImageNet dataset (Krizhevsky et al., 2012), a regularization parameter  $\lambda = 1$  and a Gaussian kernel with bandwidth  $\sigma = 10$ . The tSNE embedding method is then used to embed these representations into 2-D space utilizing the distance measures given by the UKP pseudometric. Concurrently, we perform an agglomerative (bottom-up) hierarchical clustering of the representations based on the pairwise UKP distances and obtain the corresponding dendrogram. We observe in Fig. 2 that similar architectures which share important properties, such as the Regnets and Resnets are clustered together, while they are well separated from smaller efficient architectures such as MobileNets and ConvNexTs. This demonstrates that the UKP distance effectively captures notions of similarity and dissimilarity aligned with interpretable notions based on inductive biases. Further comparisons with baseline measures, such as GULP and CKA, presented in Fig. 9 in Section A.2.2 of the Appendix demonstrate that UKP often provides superior clustering quality. We would like to note here that the choice of the kernel function for the UKP pseudometric should be driven by the nature of inductive bias that will be useful for the tasks for which the representations/features of interest will be used. Additional discussion regarding kernel (and kernel parameter) selection is provide in Section A.2.2 of the Appendix.

## 6. Conclusion and future work

This paper introduces the UKP pseudometric, a novel method for comparing model representations based on their predictive performance in kernel ridge regression tasks. It is shown to be easily interpretable, efficient, and capable of encoding inductive biases, supported by theoretical proofs and experimental validation. Therefore, the UKP pseudometric can serve as an useful and versatile exploratory tool for comparison of model representations, including representations learnt by black-box models such as neural networks, deep learning models and Large Language Models (LLMs). Future research could focus on using UKP for model selection, hyperparameter tuning, and enhancing its computational efficiency for large-scale models, such as deep neural networks, to better suit real-world applications.

## Impact Statement

This paper presents work whose goal is to advance the field of Machine Learning. There are many potential societal consequences of our work, none which we feel must be specifically highlighted here.

**References**

- 440 Aronszajn, N. Theory of reproducing kernels. *Transactions  
441 of the American Mathematical Society*, 68(3):337–404,  
442 1950.
- 443 Bengio, Y., Courville, A., and Vincent, P. Representation  
444 learning: A review and new perspectives. *IEEE Transactions  
445 on Pattern Analysis and Machine Intelligence*, 35  
446 (8):1798–1828, 2013.
- 447 Berlinet, A. and Thomas-Agnan, C. *Reproducing kernel  
448 Hilbert spaces in Probability and Statistics*. Springer  
449 Science & Business Media, 2011.
- 450 Boix-Adsera, E., Lawrence, H., Stepaniants, G., and Rigollet, P. GULP: A prediction-based metric between  
451 representations. In Koyejo, S., Mohamed, S., Agarwal, A.,  
452 Belgrave, D., Cho, K., and Oh, A. (eds.), *Advances in  
453 Neural Information Processing Systems*, volume 35, pp.  
454 7115–7127. Curran Associates, Inc., 2022.
- 455 Burnham, K. P., Anderson, D. R., Burnham, K. P., and An-  
456 derson, D. R. *Practical use of the Information-Theoretic  
457 Approach*. Springer, 1998.
- 458 Caruana, R. and Niculescu-Mizil, A. An empirical compari-  
459 son of supervised learning algorithms. In *Proceedings of  
460 the 23rd International Conference on Machine Learning*,  
461 pp. 161–168, 2006.
- 462 Cristianini, N., Shawe-Taylor, J., Elisseeff, A., and Kan-  
463 dola, J. On kernel-target alignment. *Advances in Neural  
464 Information Processing Systems*, 14, 2001.
- 465 Deng, L. The MNIST database of handwritten digit images  
466 for machine learning research [best of the web]. *IEEE  
467 Signal Processing Magazine*, 29(6):141–142, 2012.
- 468 Fernández-Delgado, M., Cernadas, E., Barro, S., and  
469 Amorim, D. Do we need hundreds of classifiers to solve  
470 real world classification problems? *The Journal of Ma-  
471 chine Learning Research*, 15(1):3133–3181, 2014.
- 472 He, K., Zhang, X., Ren, S., and Sun, J. Delving deep  
473 into rectifiers: Surpassing human-level performance on  
474 imangenet classification. In *Proceedings of the IEEE inter-  
475 national conference on computer vision*, pp. 1026–1034,  
476 2015.
- 477 Howard, A., Park, E., and Kan, W. Im-  
478 agenet object localization challenge.  
479 [https://kaggle.com/competitions/  
480 imangenet-object-localization-challenge](https://kaggle.com/competitions/imagenet-object-localization-challenge), 2018. Kaggle.
- 481 Kornblith, S., Norouzi, M., Lee, H., and Hinton, G. Similar-  
482 ity of neural network representations revisited. In *Inter-  
483 national Conference on Machine Learning*, pp. 3519–3529.  
484 PMLR, 2019.
- 485 Krizhevsky, A., Sutskever, I., and Hinton, G. E. Imagenet  
486 classification with deep convolutional neural networks.  
487 *Advances in Neural Information Processing Systems*, 25,  
488 2012.
- 489 Laakso, A. and Cottrell, G. Content and cluster analysis:  
490 Assessing representational similarity in neural systems.  
491 *Philosophical psychology*, 13(1):47–76, 2000.
- 492 LeCun, Y., Bengio, Y., and Hinton, G. Deep learning. *Nature*,  
493 521(7553):436–444, 2015.
- 494 Li, Y., Yosinski, J., Clune, J., Lipson, H., and Hopcroft,  
495 J. Convergent learning: Do different neural net-  
496 works learn the same representations? *arXiv preprint  
497 arXiv:1511.07543*, 2015.
- 498 Maurer, A., Pontil, M., and Romera-Paredes, B. The benefit  
499 of multitask representation learning. *Journal of Machine  
500 Learning Research*, 17(81):1–32, 2016.
- 501 M.Kuss and Graepel, T. The geometry of kernel canonical  
502 correlation analysis. 2003.
- 503 Morcos, A., Raghu, M., and Bengio, S. Insights on repre-  
504 sentational similarity in neural networks with canonical  
505 correlation. *Advances in Neural Information Processing  
506 Systems*, 31, 2018.
- 507 Paulsen, V. I. and Raghupathi, M. *An Introduction to the  
508 Theory of Reproducing Kernel Hilbert Spaces*, volume 152.  
509 Cambridge university press, 2016.
- 510 Pfahringer, B., Bensusan, H., and Giraud-Carrier, C. G.  
511 Meta-learning by landmarking various learning algo-  
512 rithms. In *International Conference on Machine Learn-  
513 ing*, pp. 743–750, 2000.
- 514 PyTorch. Models and pre-trained weights.  
[https://pytorch.org/vision/stable/  
515 models.html#classification](https://pytorch.org/vision/stable/models.html#classification), 2024. Accessed:  
2024-10-17.
- 516 Reed, M. and Simon, B. *Methods of Modern Mathematical  
517 Physics: Functional Analysis*, volume 1. Gulf Profes-  
518 sional Publishing, 1980.
- 519 Spiegelhalter, D. J., Best, N. G., Carlin, B. P., and Van  
520 Der Linde, A. Bayesian measures of model complexity  
521 and fit. *Journal of the Royal Statistical Society: Series B  
522 (Statistical Methodology)*, 64(4):583–639, 2002.
- 523 Sriperumbudur, B. K. and Sterge, N. Approximate kernel  
524 PCA: Computational versus statistical trade-off. *The  
525 Annals of Statistics*, 50(5):2713–2736, 2022.
- 526 Steinwart, I. and Christmann, A. *Support Vector Machines*.  
Springer Science & Business Media, 2008.

- 495 Vinod, H. D. Canonical ridge and econometrics of joint pro-  
496 duction. *Journal of Econometrics*, 4(2):147–166, 1976.  
497  
498 Wang, L., Hu, L., Gu, J., Hu, Z., Wu, Y., He, K., and  
499 Hopcroft, J. Towards understanding learning representa-  
500 tions: To what extent do different neural networks learn  
501 the same representation. *Advances in Neural Information  
502 Processing Systems*, 31, 2018.  
503  
504  
505  
506  
507  
508  
509  
510  
511  
512  
513  
514  
515  
516  
517  
518  
519  
520  
521  
522  
523  
524  
525  
526  
527  
528  
529  
530  
531  
532  
533  
534  
535  
536  
537  
538  
539  
540  
541  
542  
543  
544  
545  
546  
547  
548  
549

## A. Appendix

### A.1. Proofs of results in main paper

#### A.1.1. PROOF OF LEMMA 1

*Proof.* Consider a fixed population regression function  $\eta(x) = \mathbb{E}(Y | X = x)$  corresponding to a fixed joint distribution of  $(X, Y)$ .

Note that, for any  $f \in \mathcal{H}_\phi$ , we have

$$\begin{aligned} & \mathbb{E}[Y - f(X)]^2 + \lambda \|f\|_{\mathcal{H}_\phi}^2 \\ &= \mathbb{E}\left[Y - \langle f, K_\phi(\cdot, X) \rangle_{\mathcal{H}_\phi}\right]^2 + \lambda \|f\|_{\mathcal{H}_\phi}^2 \\ &= \mathbb{E}(Y^2) - 2\mathbb{E}\left[Y \langle f, K_\phi(\cdot, X) \rangle_{\mathcal{H}_\phi}\right] + \mathbb{E}\left[\langle f, K_\phi(\cdot, X) \rangle_{\mathcal{H}_\phi}^2\right] + \lambda \|f\|_{\mathcal{H}_\phi}^2 \\ &= \mathbb{E}(Y^2) - 2\mathbb{E}\left[\eta(X) \langle f, K_\phi(\cdot, X) \rangle_{\mathcal{H}_\phi}\right] + \mathbb{E}\langle f, [K_\phi(\cdot, X) \otimes_{\mathcal{H}_\phi} K_\phi(\cdot, X)] f \rangle_{L^2(\mathcal{H}_\phi)} + \lambda \langle f, f \rangle_{\mathcal{H}_\phi} \\ &= \mathbb{E}(Y^2) - 2\langle f, \mathfrak{J}_\phi^* \eta \rangle_{\mathcal{H}_\phi} + \langle f, (\Sigma_\phi + \lambda I)f \rangle_{\mathcal{H}_\phi} \\ &= \mathbb{E}(Y^2) + \left\|(\Sigma_\phi + \lambda I)^{\frac{1}{2}} f - (\Sigma_\phi + \lambda I)^{-\frac{1}{2}} \mathfrak{J}_\phi^* \eta\right\|_{\mathcal{H}_\phi}^2 - \left\|(\Sigma_\phi + \lambda I)^{-\frac{1}{2}} \mathfrak{J}_\phi^* \eta\right\|_{\mathcal{H}_\phi}^2. \end{aligned}$$

Therefore, the kernel ridge regression estimator of  $\eta$  using the representation  $\phi(X)$  is given by

$$\begin{aligned} \alpha_\lambda &= \arg \min_{\alpha \in \mathcal{H}_\phi} \mathbb{E}[Y - \alpha(X)]^2 + \lambda \|\alpha\|_{\mathcal{H}_\phi}^2 \\ &= \Sigma_\phi^{-\lambda} \mathfrak{J}_\phi^* \eta. \end{aligned}$$

Similarly, we can show that

$$\begin{aligned} \beta_\lambda &= \arg \min_{\beta \in \mathcal{H}_\psi} \mathbb{E}[Y - \beta(X)]^2 + \lambda \|\beta\|_{\mathcal{H}_\psi}^2 \\ &= \Sigma_\psi^{-\lambda} \mathfrak{J}_\psi^* \eta. \end{aligned}$$

Now,

$$\begin{aligned} \alpha_\lambda(x') &= \int \eta(x) \left[ \Sigma_\phi^{-\lambda} K_\phi(\cdot, x) \right] (x') dP_X(x) \\ &= \int \eta(x) \left\langle \Sigma_\phi^{-\lambda} K_\phi(\cdot, x), K_\phi(\cdot, x') \right\rangle_{\mathcal{H}_\phi} dP_X(x) \\ &= \int \eta(x) \left\langle \Sigma_\phi^{-\frac{\lambda}{2}} K_\phi(\cdot, x), \Sigma_\phi^{-\frac{\lambda}{2}} K_\phi(\cdot, x') \right\rangle_{\mathcal{H}_\phi} dP_X(x) \\ &= \left\langle \eta, \left\langle \Sigma_\phi^{-\frac{\lambda}{2}} K_\phi(\cdot, x), \Sigma_\phi^{-\frac{\lambda}{2}} K_\phi(\cdot, x') \right\rangle_{\mathcal{H}_\phi} \right\rangle_{L^2(P_X)} \\ &= \left\langle \eta, \left\langle \tilde{K}_\phi(\cdot, x), \tilde{K}_\phi(\cdot, x') \right\rangle_{\mathcal{H}_\phi} \right\rangle_{L^2(P_X)} \\ &= \left\langle \eta, \left\langle \tilde{K}_\phi(\cdot, x), \tilde{K}_\phi(\cdot, x') \right\rangle_{\mathcal{H}} \right\rangle_{L^2(P_X)}. \end{aligned}$$

Similarly,

$$\begin{aligned} \beta_\lambda(x') &= \left\langle \eta, \left\langle \tilde{K}_\psi(\cdot, x), \tilde{K}_\psi(\cdot, x') \right\rangle_{\mathcal{H}_\psi} \right\rangle_{L^2(P_X)} \\ &= \left\langle \eta, \left\langle \tilde{K}_\psi(\cdot, x), \tilde{K}_\psi(\cdot, x') \right\rangle_{\mathcal{H}} \right\rangle_{L^2(P_X)}. \end{aligned}$$

605 Therefore, we have that

$$\begin{aligned}
 [d_{\lambda,K}^{\text{UKP}}(\phi, \psi)]^2 &= \sup_{\|\eta\|_{L^2(P_X)} \leq 1} \mathbb{E} [\alpha_\lambda(X) - \beta_\lambda(X)]^2 \\
 &= \sup_{\|\eta\|_{L^2(P_X)} \leq 1} \mathbb{E} \left\langle \eta, \left\langle \tilde{K}_\phi(\cdot, \cdot), \tilde{K}_\phi(\cdot, X) \right\rangle_{\mathcal{H}_\phi} - \left\langle \tilde{K}_\psi(\cdot, \cdot), \tilde{K}_\psi(\cdot, X) \right\rangle_{\mathcal{H}_\psi} \right\rangle_{L^2(P_X)}^2 \\
 &= \mathbb{E} \left\| \left\langle \tilde{K}_\phi(\cdot, \cdot), \tilde{K}_\phi(\cdot, X) \right\rangle_{\mathcal{H}_\phi} - \left\langle \tilde{K}_\psi(\cdot, \cdot), \tilde{K}_\psi(\cdot, X) \right\rangle_{\mathcal{H}_\psi} \right\|_{L^2(P_X)}^2 \\
 &= \mathbb{E} \left[ \left\langle \Sigma_\phi^{-\frac{\lambda}{2}} K_\phi(\cdot, X), \Sigma_\phi^{-\frac{\lambda}{2}} K_\phi(\cdot, X') \right\rangle_{\mathcal{H}_\phi} - \left\langle \Sigma_\psi^{-\frac{\lambda}{2}} K_\psi(\cdot, X), \Sigma_\psi^{-\frac{\lambda}{2}} K_\psi(\cdot, X') \right\rangle_{\mathcal{H}_\psi} \right]^2 \\
 &= \mathbb{E} \left[ \left\langle K_\phi(\cdot, X), \Sigma_\phi^{-\lambda} K_\phi(\cdot, X') \right\rangle_{\mathcal{H}_\phi} - \left\langle K_\psi(\cdot, X), \Sigma_\psi^{-\lambda} K_\psi(\cdot, X') \right\rangle_{\mathcal{H}_\psi} \right]^2
 \end{aligned}$$

622 where  $X$  and  $X'$  are i.i.d observations drawn from  $P_X$ . □

### A.1.2. PROOF OF PROPOSITION 1

630 *Proof.* Using Lemma 1, the squared UKP distance of  $d_{\lambda,K}^{\text{UKP}}(\phi, \psi)$  between representations  $\phi(X)$  and  $\psi(X)$  can be  
631 expressed as

$$\begin{aligned}
 [d_{\lambda,K}^{\text{UKP}}(\phi, \psi)]^2 &= \mathbb{E} \left[ \left\langle \tilde{K}_\phi(\cdot, X), \tilde{K}_\phi(\cdot, X') \right\rangle_{\mathcal{H}_\phi} - \left\langle \tilde{K}_\psi(\cdot, X), \tilde{K}_\psi(\cdot, X') \right\rangle_{\mathcal{H}_\psi} \right]^2 \\
 &= \mathbb{E} \left[ \left\langle \tilde{K}_\phi(\cdot, X) \otimes_{\mathcal{H}_\phi} \tilde{K}_\phi(\cdot, X), \tilde{K}_\phi(\cdot, X') \otimes_{\mathcal{H}_\phi} \tilde{K}_\phi(\cdot, X') \right\rangle_{\mathcal{L}^2(\mathcal{H}_\phi)} \right. \\
 &\quad \left. + \left\langle \tilde{K}_\psi(\cdot, X) \otimes_{\mathcal{H}_\psi} \tilde{K}_\psi(\cdot, X), \tilde{K}_\psi(\cdot, X') \otimes_{\mathcal{H}_\psi} \tilde{K}_\psi(\cdot, X') \right\rangle_{\mathcal{L}^2(\mathcal{H}_\psi)} \right. \\
 &\quad \left. - 2 \left\langle \tilde{K}_\phi(\cdot, X) \otimes_{\mathcal{L}^2(\mathcal{H}_\psi, \mathcal{H}_\phi)} \tilde{K}_\psi(\cdot, X), \tilde{K}_\phi(\cdot, X') \otimes_{\mathcal{L}^2(\mathcal{H}_\psi, \mathcal{H}_\phi)} \tilde{K}_\psi(\cdot, X') \right\rangle_{\mathcal{L}^2(\mathcal{H}_\psi, \mathcal{H}_\phi)} \right] \\
 &= \left\langle \Sigma_\phi^{-\frac{\lambda}{2}} \Sigma_\phi \Sigma_\phi^{-\frac{\lambda}{2}}, \Sigma_\phi^{-\frac{\lambda}{2}} \Sigma_\phi \Sigma_\phi^{-\frac{\lambda}{2}} \right\rangle_{\mathcal{L}^2(\mathcal{H}_\phi)} + \left\langle \Sigma_\psi^{-\frac{\lambda}{2}} \Sigma_\psi \Sigma_\psi^{-\frac{\lambda}{2}}, \Sigma_\psi^{-\frac{\lambda}{2}} \Sigma_\psi \Sigma_\psi^{-\frac{\lambda}{2}} \right\rangle_{\mathcal{L}^2(\mathcal{H}_\psi)} \\
 &\quad - 2 \left\langle \Sigma_\phi^{-\frac{\lambda}{2}} \Sigma_{\phi\psi} \Sigma_\psi^{-\frac{\lambda}{2}}, \Sigma_\phi^{-\frac{\lambda}{2}} \Sigma_{\phi\psi} \Sigma_\psi^{-\frac{\lambda}{2}} \right\rangle_{\mathcal{L}^2(\mathcal{H}_\psi, \mathcal{H}_\phi)} \\
 &= \text{Tr} \left( \Sigma_\phi^{-\lambda} \Sigma_\phi \Sigma_\phi^{-\lambda} \Sigma_\phi \right) + \text{Tr} \left( \Sigma_\psi^{-\lambda} \Sigma_\psi \Sigma_\psi^{-\lambda} \Sigma_\psi \right) - 2 \text{Tr} \left( \Sigma_\phi^{-\lambda} \Sigma_{\phi\psi} \Sigma_\psi^{-\lambda} \Sigma_{\psi\phi} \right)
 \end{aligned}$$

651 which completes the proof. □

### A.1.3. PROOF OF THEOREM 1

658 *Proof.* The first three properties immediately follow from the characterization of  $d_{\lambda,K}^{\text{UKP}}$  given in Lemma 1.  
659

660 Note that,

$$\begin{aligned}
 d_{\lambda,K}^{\text{UKP}}(\phi, \psi) &= \left( \mathbb{E} \left[ \left\langle K_\phi(\cdot, X), \Sigma_\phi^{-\lambda} K_\phi(\cdot, X') \right\rangle_{\mathcal{H}_\phi} - \left\langle K_\psi(\cdot, X), \Sigma_\psi^{-\lambda} K_\psi(\cdot, X') \right\rangle_{\mathcal{H}_\psi} \right]^2 \right)^{\frac{1}{2}} \\
 &= \left( \mathbb{E} \left[ \left\langle K_\phi(\cdot, X), \Sigma_\phi^{-\lambda} K_\phi(\cdot, X') \right\rangle_{\mathcal{H}_\phi} - \left\langle K_\varphi(\cdot, X), \Sigma_\varphi^{-\lambda} K_\varphi(\cdot, X') \right\rangle_{\mathcal{H}_\varphi} \right. \right. \\
 &\quad \left. \left. + \left\langle K_\varphi(\cdot, X), \Sigma_\varphi^{-\lambda} K_\varphi(\cdot, X') \right\rangle_{\mathcal{H}_\varphi} - \left\langle K_\psi(\cdot, X), \Sigma_\psi^{-\lambda} K_\psi(\cdot, X') \right\rangle_{\mathcal{H}_\psi} \right]^2 \right)^{\frac{1}{2}} \\
 &\stackrel{\dagger}{\leq} \left( \mathbb{E} \left[ \left\langle K_\phi(\cdot, X), \Sigma_\phi^{-\lambda} K_\phi(\cdot, X') \right\rangle_{\mathcal{H}_\phi} - \left\langle K_\varphi(\cdot, X), \Sigma_\varphi^{-\lambda} K_\varphi(\cdot, X') \right\rangle_{\mathcal{H}_\varphi} \right]^2 \right)^{\frac{1}{2}} \\
 &\quad + \left( \mathbb{E} \left[ \left\langle K_\varphi(\cdot, X), \Sigma_\varphi^{-\lambda} K_\varphi(\cdot, X') \right\rangle_{\mathcal{H}_\varphi} - \left\langle K_\psi(\cdot, X), \Sigma_\psi^{-\lambda} K_\psi(\cdot, X') \right\rangle_{\mathcal{H}_\psi} \right]^2 \right)^{\frac{1}{2}} \\
 &= d_{\lambda,K}^{\text{UKP}}(\phi, \varphi) + d_{\lambda,K}^{\text{UKP}}(\varphi, \psi),
 \end{aligned}$$

677 where  $\dagger$  follows using Minkowski's inequality for integrals. Thus, the  $d_{\lambda,K}^{\text{UKP}}$  distance satisfies the triangle inequality along  
 678 with the other three properties, and consequently, fulfills all the requirements of a pseudometric.  $\square$

#### 680 A.1.4. PROOF OF LEMMA 2

682 *Proof.* The sufficiency of the condition is obvious, so we proceed to prove the necessity part.

683 Under the given conditions on the kernel  $K$ , the integral operators  $\mathcal{T}_f$  and  $\mathcal{T}_g$  corresponding to the kernels  $K_f$  and  $K_g$  both  
 684 admit spectral decompositions. Let  $(\mu_i^f, e_i^f)_{i=1}^\infty$  and  $(\mu_j^g, e_j^g)_{j=1}^\infty$  be the eigenvalue-eigenfunction pairs corresponding to  
 685 the spectral decomposition of  $\mathcal{T}_f$  and  $\mathcal{T}_g$ , respectively. Then, we have that

$$\mathcal{T}_f = \sum_{i=1}^{\infty} \mu_i^f (e_i^f \otimes_{L^2(P_X)} e_i^f)$$

690 and

$$\mathcal{T}_g = \sum_{j=1}^{\infty} \mu_j^g (e_j^g \otimes_{L^2(P_X)} e_j^g).$$

694 Since  $K$  is a positive definite, symmetric, continuous and bounded kernel defined on a separable domain,  $\mathcal{T}_f$  and  $\mathcal{T}_g$  are  
 695 compact, self-adjoint, trace-class operators. Therefore, we must have that  $\mu_i^f, \mu_j^g > 0$  and  $\lim_{i \rightarrow \infty} \mu_i^f = \lim_{j \rightarrow \infty} \mu_j^g = 0$ .  
 696 Further,  $(e_i^f)_{i=1}^\infty$  and  $(e_j^g)_{j=1}^\infty$  constitute orthonormal bases of  $\mathcal{H}_f$  and  $\mathcal{H}_g$ , respectively.

698 The Mercer decompositions of the kernels  $K_f$  and  $K_g$  are given by,

$$\mathcal{K}_f(x, x') = \sum_{i=1}^{\infty} \mu_i^f e_i^f(x) e_i^f(x')$$

703 and

$$\mathcal{K}_g(x, x') = \sum_{j=1}^{\infty} \mu_j^g e_j^g(x) e_j^g(x').$$

707 Note that,

$$\begin{aligned}
 \mathcal{I}(f)(x, x') &= \left\langle \Sigma_f^{-\frac{\lambda}{2}} K_f(\cdot, x), \Sigma_f^{-\frac{\lambda}{2}} K_f(\cdot, x') \right\rangle_{\mathcal{H}_f} \\
 &= \left\langle K_f(\cdot, x), \Sigma_f^{-\lambda} K_f(\cdot, x') \right\rangle_{\mathcal{H}_f} \\
 &= \sum_{i=1}^{\infty} \frac{\mu_i^f}{\mu_i^f + \lambda} e_i^f(x) e_i^f(x').
 \end{aligned} \tag{4}$$

715 Similarly, we have

$$716 \quad 717 \quad 718 \quad 719 \quad 720 \quad 721 \quad 722 \quad 723 \quad 724 \quad 725 \quad 726 \quad 727 \quad 728 \quad 729 \quad 730 \quad 731 \quad 732 \quad 733 \quad 734 \quad 735 \quad 736 \quad 737 \quad 738 \quad 739 \quad 740 \quad 741 \quad 742 \quad 743 \quad 744 \quad 745 \quad 746 \quad 747 \quad 748 \quad 749 \quad 750 \quad 751 \quad 752 \quad 753 \quad 754 \quad 755 \quad 756 \quad 757 \quad 758 \quad 759 \quad 760 \quad 761 \quad 762 \quad 763 \quad 764 \quad 765 \quad 766 \quad 767 \quad 768 \quad 769$$

$$\mathcal{I}(g)(x, x') = \sum_{j=1}^{\infty} \frac{\mu_j^g}{\mu_j^g + \lambda} e_j^g(x) e_j^g(x'). \quad (5)$$

Define  $t_{ij} := \langle e_i^f, e_j^g \rangle_{L^2(P_X)}$  for all  $i, j$ . Further, define  $V_i = \{j \in \mathbb{N} : t_{ij} \neq 0\}$  for all  $i$  and  $W_j = \{i \in \mathbb{N} : t_{ij} \neq 0\}$  for all  $j$ . Now, using (4) and (5), we have that

$$\begin{aligned} & \mathcal{I}(f) = \mathcal{I}(g) \\ \iff & \sum_{i=1}^{\infty} \frac{\mu_i^f}{\mu_i^f + \lambda} e_i^f(\cdot) e_i^f(\cdot) = \sum_{j=1}^{\infty} \frac{\mu_j^g}{\mu_j^g + \lambda} e_j^g(\cdot) e_j^g(\cdot). \end{aligned} \quad (6)$$

Taking the  $L^2(P_X)$  inner product of both the RHS and LHS of (6) with  $e_j^g$ , we have that

$$\sum_{i=1}^{\infty} \frac{\mu_i^f t_{ij}}{\mu_i^f + \lambda} e_i^f(\cdot) = \frac{\mu_j^g}{\mu_j^g + \lambda} e_j^g(\cdot). \quad (7)$$

Taking the  $L^2(P_X)$  inner product of both the RHS and LHS of (7) with  $e_k^f$ , we have that

$$\begin{aligned} & \frac{\mu_k^f t_{kj}}{\mu_k^f + \lambda} = \frac{\mu_j^g t_{kj}}{\mu_j^g + \lambda} \\ \iff & t_{kj} \left( \frac{\mu_k^f}{\mu_k^f + \lambda} - \frac{\mu_j^g}{\mu_j^g + \lambda} \right) = 0 \\ \iff & t_{kj} (\mu_k^f - \mu_j^g) = 0. \end{aligned} \quad (8)$$

Taking the  $L^2(P_X)$  inner product of both the RHS and LHS of (7) with  $e_k^g$ , we have that

$$\begin{aligned} & \sum_{i=1}^{\infty} \frac{\mu_i^f t_{ij} t_{ik}}{\mu_i^f + \lambda} = \begin{cases} \frac{\mu_j^g}{\mu_j^g + \lambda} & \text{if } j = k \\ 0, & \text{if } j \neq k \end{cases} \\ \iff & \sum_{i \in W_j \cap W_k} \frac{\mu_i^f t_{ij} t_{ik}}{\mu_i^f + \lambda} = \begin{cases} \frac{\mu_j^g}{\mu_j^g + \lambda} & \text{if } j = k \\ 0, & \text{if } j \neq k \end{cases}. \end{aligned} \quad (9)$$

Using (8) and (9), we have that

$$\frac{\mu_j^g}{\mu_j^g + \lambda} \left[ \sum_{i \in W_j} t_{ij}^2 - 1 \right] = 0 \quad (10)$$

and, if  $j \neq k$ ,

$$\frac{\mu_j^g}{\mu_j^g + \lambda} \left( \sum_{i \in W_j \cap W_k} t_{ij} t_{ik} \right) = 0. \quad (11)$$

Therefore, from (10) and (11), we obtain that

$$\sum_{i \in W_j} t_{ij}^2 = 1 \quad (12)$$

and, if  $j \neq k$ ,

$$\sum_{i \in W_j \cap W_k} t_{ij} t_{ik} = 0. \quad (13)$$

770 In exactly analogous manner, we can also obtain

$$771 \quad \sum_{j \in V_i} t_{ij}^2 = 1 \quad (14)$$

772 and, if  $i \neq k$ ,

$$773 \quad \sum_{j \in V_i \cap V_k} t_{ij} t_{kj} = 0. \quad (15)$$

774 Note that  $(e_j^g)_{j=1}^\infty$  can be extended to obtain an orthonormal basis for  $L^2(P_X)$ . Let  $B = \{\cup_{j=1}^\infty e_j^g\} \cup \{\cup_{l=1}^\infty z_l^g\}$  be the  
775 resulting orthonormal basis of  $L^2(P_X)$  obtained by said extension.

776 Now,

$$777 \quad e_i^f = \sum_{j=1}^\infty \langle e_i^f, e_j^g \rangle e_j^g + \sum_{l=1}^\infty \langle e_i^f, z_l^g \rangle z_l^g. \quad (16)$$

778 Therefore, using (16) and (14) along with the orthonormality of  $(e_i^f)_{i=1}^\infty$ , we have,

$$\begin{aligned} 779 \quad & \|e_i^f\|_{L^2(P_X)} = 1 \\ 780 \quad & \iff \sum_{j=1}^\infty \langle e_i^f, e_j^g \rangle^2 + \sum_{l=1}^\infty \langle e_i^f, z_l^g \rangle^2 = 1 \\ 781 \quad & \iff \sum_{j \in V_i} t_{ij}^2 + \sum_{l=1}^\infty \langle e_i^f, z_l^g \rangle^2 = 1 \\ 782 \quad & \iff \sum_{l=1}^\infty \langle e_i^f, z_l^g \rangle^2 = 0 \\ 783 \quad & \iff \langle e_i^f, z_l^g \rangle = 0 \text{ for all } l \text{ and } i. \end{aligned}$$

800 Hence, for all  $i$ ,  $e_i^f \in \text{Span}\{e_j^g, j \in \mathbb{N}\}$ . Consequently,  $\mathcal{T}_f e_j^g = \sum_{i=1}^\infty \mu_i^f t_{ij} e_i^f \in \text{Span}\{e_i^f, i \in \mathbb{N}\} \subset \text{Span}\{e_j^g, j \in \mathbb{N}\}$ .

801 Now, using (13) and (8), for any  $j \neq k$ , we have

$$\begin{aligned} 802 \quad & \langle \mathcal{T}_f e_j^g, e_k^g \rangle_{L^2(P_X)} = \sum_{i=1}^\infty \mu_i^f t_{ij} t_{ik} \\ 803 \quad & = \sum_{i \in W_j \cap W_k} \mu_i^f t_{ij} t_{ik} \\ 804 \quad & = \mu_j^g \sum_{i \in W_j \cap W_k} t_{ij} t_{ik} \\ 805 \quad & = 0. \end{aligned}$$

813 Finally, using (10) and (8), we have that

$$\begin{aligned} 814 \quad & \langle \mathcal{T}_f e_j^g, e_j^g \rangle_{L^2(P_X)} = \sum_{i=1}^\infty \mu_i^f t_{ij}^2 \\ 815 \quad & = \sum_{i \in W_j} \mu_i^f t_{ij}^2 \\ 816 \quad & = \mu_j^g \sum_{i \in W_j} t_{ij}^2 \\ 817 \quad & = \mu_j^g > 0. \end{aligned}$$

825 Therefore,  $\mathcal{T}_f e_j^g = \mu_j^g e_j^g$  for all  $j$ . Therefore, all the eigenfunctions of  $\mathcal{T}_g$  are also eigenfunctions of  $\mathcal{T}_f$ . By symmetry, all  
 826 the eigenfunctions of  $\mathcal{T}_f$  are also eigenfunctions of  $\mathcal{T}_g$ . Therefore,  $\mathcal{T}_f$  and  $\mathcal{T}_g$  have exactly the same eigenfunctions.  
 827

828 Consequently, (6) can be now written as

$$\begin{aligned} 829 \quad & \mathcal{I}(f) = \mathcal{I}(g) \\ 830 \quad & \iff \sum_{i=1}^{\infty} \frac{\mu_i^f}{\mu_i^f + \lambda} e_i^f(\cdot) e_i^f(\cdot) = \sum_{i=1}^{\infty} \frac{\mu_i^g}{\mu_i^g + \lambda} e_i^g(\cdot) e_i^g(\cdot). \end{aligned} \quad (17)$$

834 Taking the  $L^2(P_X)$  inner product of both the RHS and LHS of (17) with  $e_i^f$  twice, we have that, for any  $i$ ,

$$\begin{aligned} 837 \quad & \frac{\mu_i^f}{\mu_i^f + \lambda} = \frac{\mu_i^g}{\mu_i^g + \lambda} \\ 838 \quad & \iff \mu_i^f = \mu_i^g. \end{aligned}$$

841 Therefore, we must have that the integral operators  $\mathcal{T}_f$  and  $\mathcal{T}_g$  have the same spectral decomposition. Consequently, their  
 842 corresponding kernel functions and RKHS's must be the same. Therefore, we must have  $K_f(\cdot, \cdot) = K_g(\cdot, \cdot)$ . This concludes  
 843 the proof of the necessity part and consequently, the proof of Lemma 2.  $\square$

#### A.1.5. PROOF OF COROLLARY 1

844 *Proof.* Define the operator  $\mathcal{I}$  as in Lemma 2. Then, we have that, for any  $h_1, h_2 \in \mathcal{H}$

$$\begin{aligned} 845 \quad & d_{\lambda, K}^{\text{UKP}}(h_1 \circ \phi, h_2 \circ \psi) \\ 846 \quad & = \left( \mathbb{E} [\mathcal{I}(h_1 \circ \phi)(X, X') - \mathcal{I}(h_2 \circ \psi)(X, X')]^2 \right)^{\frac{1}{2}} \\ 847 \quad & = \left( \mathbb{E} [\mathcal{I}(\phi)(X, X') - \mathcal{I}(\psi)(X, X')]^2 \right)^{\frac{1}{2}} \\ 848 \quad & = d_{\lambda, K}^{\text{UKP}}(\phi, \psi). \end{aligned}$$

849 If either  $h_1$  or  $h_2$  does not belong to  $\mathcal{H}$ , then using Lemma 2, we have that  $[\mathcal{I}(h_1 \circ \phi)(X, X') - \mathcal{I}(h_2 \circ \psi)(X, X')]^2$  must  
 850 be strictly positive on a set with positive measure w.r.t  $P_X$ . Therefore, we must have  $d_{\lambda, K}^{\text{UKP}}(h_1 \circ \phi, h_2 \circ \psi) > 0$ .  $\square$

#### A.1.6. PROOF OF THEOREM 2

851 *Proof.* Note that for any  $x, y \in \mathbb{R}^d$ ,  $\hat{\Sigma}_{\phi}^{-\lambda} [K_{\phi}(\cdot, x) \otimes_{\mathcal{H}_{\phi}} K_{\phi}(\cdot, x)] \hat{\Sigma}_{\phi}^{-\lambda} [K_{\phi}(\cdot, y) \otimes_{\mathcal{H}_{\phi}} K_{\phi}(\cdot, y)]$  is a rank-  
 852 one operator with eigenvalue  $\left\langle \hat{\Sigma}_{\phi}^{-\frac{\lambda}{2}} K_{\phi}(\cdot, x), \hat{\Sigma}_{\phi}^{-\frac{\lambda}{2}} K_{\phi}(\cdot, y) \right\rangle_{\mathcal{H}_{\phi}}^2$  and eigenfunction  $\frac{\hat{\Sigma}_{\phi}^{-\lambda} K_{\phi}(\cdot, x)}{\|\hat{\Sigma}_{\phi}^{-\lambda} K_{\phi}(\cdot, x)\|_{\mathcal{H}_{\phi}}}$ . Sim-  
 853ilarly,  $\hat{\Sigma}_{\psi}^{-\lambda} [K_{\psi}(\cdot, x) \otimes_{\mathcal{H}_{\psi}} K_{\psi}(\cdot, x)] \hat{\Sigma}_{\psi}^{-\lambda} [K_{\psi}(\cdot, y) \otimes_{\mathcal{H}_{\psi}} K_{\psi}(\cdot, y)]$  is a rank-one operator with eigenvalue  
 854  $\left\langle \hat{\Sigma}_{\psi}^{-\frac{\lambda}{2}} K_{\psi}(\cdot, x), \hat{\Sigma}_{\psi}^{-\frac{\lambda}{2}} K_{\psi}(\cdot, y) \right\rangle_{\mathcal{H}_{\psi}}^2$  and eigenfunction  $\frac{\hat{\Sigma}_{\psi}^{-\lambda} K_{\psi}(\cdot, x)}{\|\hat{\Sigma}_{\psi}^{-\lambda} K_{\psi}(\cdot, x)\|_{\mathcal{H}_{\psi}}}$ . Further,  $\hat{\Sigma}_{\phi}^{-\lambda} [K_{\phi}(\cdot, x) \otimes_{\mathcal{L}^2(\mathcal{H}_{\phi}, \mathcal{H}_{\psi})} K_{\psi}(\cdot, x)] \times$   
 855  $\hat{\Sigma}_{\psi}^{-\lambda} [K_{\psi}(\cdot, y) \otimes_{\mathcal{L}^2(\mathcal{H}_{\phi}, \mathcal{H}_{\psi})} K_{\phi}(\cdot, y)]$  is a rank-one operator with eigenvalue  $\left\langle \hat{\Sigma}_{\phi}^{-\frac{\lambda}{2}} K_{\phi}(\cdot, x), \hat{\Sigma}_{\phi}^{-\frac{\lambda}{2}} K_{\phi}(\cdot, y) \right\rangle_{\mathcal{H}_{\phi}} \times$   
 856  $\left\langle \hat{\Sigma}_{\psi}^{-\frac{\lambda}{2}} K_{\psi}(\cdot, x), \hat{\Sigma}_{\psi}^{-\frac{\lambda}{2}} K_{\psi}(\cdot, y) \right\rangle_{\mathcal{H}_{\psi}}$  and eigenfunction  $\frac{\hat{\Sigma}_{\phi}^{-\lambda} K_{\phi}(\cdot, x)}{\|\hat{\Sigma}_{\phi}^{-\lambda} K_{\phi}(\cdot, x)\|_{\mathcal{H}_{\phi}}} \cdot$

857 Using these facts, we have that the squared V-statistic type estimator of  $d_{\lambda, K}^{\text{UKP}}$  can be expressed as

$$858 \quad \left[ \hat{d}_{\lambda}^{\text{UKP}}(\phi, \psi) \right]^2 = \frac{1}{n^2} \sum_{i=1}^n \sum_{j=1}^n \left[ \left\langle \hat{\Sigma}_{\phi}^{-\frac{\lambda}{2}} K_{\phi}(\cdot, X_i), \hat{\Sigma}_{\phi}^{-\frac{\lambda}{2}} K_{\phi}(\cdot, X_j) \right\rangle_{\mathcal{H}_{\phi}} - \left\langle \hat{\Sigma}_{\psi}^{-\frac{\lambda}{2}} K_{\psi}(\cdot, X_i), \hat{\Sigma}_{\psi}^{-\frac{\lambda}{2}} K_{\psi}(\cdot, X_j) \right\rangle_{\mathcal{H}_{\psi}} \right]^2.$$

Let us define the following quantity

$$\left[ \tilde{d}_\lambda^{\text{UKP}}(\phi, \psi) \right]^2 := \frac{1}{n^2} \sum_{i=1}^n \sum_{j=1}^n \left[ \left\langle \Sigma_\phi^{-\frac{\lambda}{2}} K_\phi(\cdot, X_i), \Sigma_\phi^{-\frac{\lambda}{2}} K_\phi(\cdot, X_j) \right\rangle_{\mathcal{H}_\phi} - \left\langle \Sigma_\psi^{-\frac{\lambda}{2}} K_\psi(\cdot, X_i), \Sigma_\psi^{-\frac{\lambda}{2}} K_\psi(\cdot, X_j) \right\rangle_{\mathcal{H}_\psi} \right]^2$$

which is  $\left[ \hat{d}_\lambda^{\text{UKP}}(\phi, \psi) \right]^2$  with  $\hat{\Sigma}_\phi$  and  $\hat{\Sigma}_\phi$  replaced by  $\Sigma_\phi$  and  $\Sigma_\phi$ , respectively.

We utilize the triangle inequality to bound the difference between the squared V-statistic type estimator  $\left[ \tilde{d}_\lambda^{\text{UKP}}(\phi, \psi) \right]^2$  and the squared population distance  $\left[ d_{\lambda, K}^{\text{UKP}}(\phi, \psi) \right]^2$  as follows:

$$\left| \left[ \tilde{d}_\lambda^{\text{UKP}}(\phi, \psi) \right]^2 - \left[ d_{\lambda, K}^{\text{UKP}}(\phi, \psi) \right]^2 \right| \leq \underbrace{\left| \left[ \tilde{d}_\lambda^{\text{UKP}}(\phi, \psi) \right]^2 - \left[ \tilde{d}_\lambda^{\text{UKP}}(\phi, \psi) \right]^2 \right|}_{\mathbf{A}} + \underbrace{\left| \left[ \tilde{d}_\lambda^{\text{UKP}}(\phi, \psi) \right]^2 - \left[ d_{\lambda, K}^{\text{UKP}}(\phi, \psi) \right]^2 \right|}_{\mathbf{B}}. \quad (18)$$

We now proceed to bound **A**. Let us define

$$\hat{A}_{ij, \phi} = \left\langle \hat{\Sigma}_\phi^{-\frac{\lambda}{2}} K_\phi(\cdot, X_i), \hat{\Sigma}_\phi^{-\frac{\lambda}{2}} K_\phi(\cdot, X_j) \right\rangle_{\mathcal{H}_\phi},$$

$$A_{ij, \phi} = \left\langle \Sigma_\phi^{-\frac{\lambda}{2}} K_\phi(\cdot, X_i), \Sigma_\phi^{-\frac{\lambda}{2}} K_\phi(\cdot, X_j) \right\rangle_{\mathcal{H}_\phi},$$

$$\hat{A}_{ij, \psi} = \left\langle \hat{\Sigma}_\psi^{-\frac{\lambda}{2}} K_\psi(\cdot, X_i), \hat{\Sigma}_\psi^{-\frac{\lambda}{2}} K_\psi(\cdot, X_j) \right\rangle_{\mathcal{H}_\psi},$$

$$A_{ij, \psi} = \left\langle \Sigma_\psi^{-\frac{\lambda}{2}} K_\psi(\cdot, X_i), \Sigma_\psi^{-\frac{\lambda}{2}} K_\psi(\cdot, X_j) \right\rangle_{\mathcal{H}_\psi}.$$

Then, we have that

$$\left| \hat{A}_{ij, \phi} \right| \leq \|K_\phi(\cdot, X_i)\|_{\mathcal{H}_\phi}^2 \times \left\| \hat{\Sigma}_\phi^{-\frac{\lambda}{2}} \right\|_{\mathcal{L}^\infty(\mathcal{H}_\phi)}^2 \leq \frac{\kappa}{\lambda}.$$

Similarly, we can show that  $|\hat{A}_{ij, \psi}| \leq \frac{\kappa}{\lambda}$ ,  $|A_{ij, \phi}| \leq \frac{\kappa}{\lambda}$  and  $|A_{ij, \psi}| \leq \frac{\kappa}{\lambda}$ .

Now, we have that

$$\begin{aligned} \left| \hat{A}_{ij, \phi} - A_{ij, \phi} \right| &= \left| \left\langle K_\phi(\cdot, X_i), \left( \hat{\Sigma}_\phi^{-\lambda} - \Sigma_\phi^{-\lambda} \right) K_\phi(\cdot, X_j) \right\rangle_{\mathcal{H}_\phi} \right| \\ &\leq \kappa \left\| \hat{\Sigma}_\phi^{-\lambda} - \Sigma_\phi^{-\lambda} \right\|_{\mathcal{L}^\infty(\mathcal{H}_\phi)} \\ &\leq \kappa \left\| \hat{\Sigma}_\phi^{-\lambda} - \Sigma_\phi^{-\lambda} \right\|_{\mathcal{L}^2(\mathcal{H}_\phi)}. \end{aligned}$$

Similarly, we have that

$$\begin{aligned} \left| \hat{A}_{ij, \psi} - A_{ij, \psi} \right| &= \left| \left\langle K_\psi(\cdot, X_i), \left( \hat{\Sigma}_\psi^{-\lambda} - \Sigma_\psi^{-\lambda} \right) K_\psi(\cdot, X_j) \right\rangle_{\mathcal{H}_\psi} \right| \\ &\leq \kappa \left\| \hat{\Sigma}_\psi^{-\lambda} - \Sigma_\psi^{-\lambda} \right\|_{\mathcal{L}^\infty(\mathcal{H}_\psi)} \\ &\leq \kappa \left\| \hat{\Sigma}_\psi^{-\lambda} - \Sigma_\psi^{-\lambda} \right\|_{\mathcal{L}^2(\mathcal{H}_\psi)}. \end{aligned}$$

935 Note that,

$$\begin{aligned}
 937 \quad & \left\| \hat{\Sigma}_\phi^{-\lambda} - \Sigma_\phi^{-\lambda} \right\|_{\mathcal{L}^\infty(\mathcal{H}_\phi)} = \left\| \left( \hat{\Sigma}_\phi + \lambda I \right)^{-1} (\Sigma_\phi + \lambda I) (\Sigma_\phi + \lambda I)^{-1} - \left( \hat{\Sigma}_\phi + \lambda I \right)^{-1} (\hat{\Sigma}_\phi + \lambda I) (\Sigma_\phi + \lambda I)^{-1} \right\|_{\mathcal{L}^\infty(\mathcal{H}_\phi)} \\
 938 \quad & = \left\| \hat{\Sigma}_\phi^{-\lambda} \left[ (\Sigma_\phi + \lambda I) - (\hat{\Sigma}_\phi + \lambda I) \right] \Sigma_\phi^{-\lambda} \right\|_{\mathcal{L}^\infty(\mathcal{H}_\phi)} \\
 939 \quad & \leq \left\| \hat{\Sigma}_\phi^{-\lambda} \right\|_{\mathcal{L}^\infty(\mathcal{H}_\phi)} \left\| \Sigma_\phi - \hat{\Sigma}_\phi \right\|_{\mathcal{L}^\infty(\mathcal{H}_\phi)} \left\| \Sigma_\phi^{-\lambda} \right\|_{\mathcal{L}^\infty(\mathcal{H}_\phi)} \\
 940 \quad & \leq \frac{1}{\lambda^2} \left\| \Sigma_\phi - \hat{\Sigma}_\phi \right\|_{\mathcal{L}^\infty(\mathcal{H}_\phi)} \\
 941 \quad & \leq \frac{1}{\lambda^2} \left\| \Sigma_\phi - \hat{\Sigma}_\phi \right\|_{\mathcal{L}^2(\mathcal{H}_\phi)}.
 \end{aligned}$$

$$942 \quad \text{Similarly, } \left\| \hat{\Sigma}_\psi^{-\lambda} - \Sigma_\psi^{-\lambda} \right\|_{\mathcal{L}^\infty(\mathcal{H}_\psi)} \leq \frac{1}{\lambda^2} \left\| \Sigma_\psi - \hat{\Sigma}_\psi \right\|_{\mathcal{L}^\infty(\mathcal{H}_\psi)} \leq \frac{1}{\lambda^2} \left\| \Sigma_\psi - \hat{\Sigma}_\psi \right\|_{\mathcal{L}^2(\mathcal{H}_\psi)}.$$

943 Therefore, we have that

$$\begin{aligned}
 944 \quad & \mathbf{A} = \left| \frac{1}{n^2} \sum_{i=1}^n \sum_{j=1}^n \left[ \left( \hat{A}_{ij,\phi} - \hat{A}_{ij,\psi} \right)^2 - (A_{ij,\phi} - A_{ij,\psi})^2 \right] \right| \\
 945 \quad & = \left| \frac{1}{n^2} \sum_{i=1}^n \sum_{j=1}^n \left[ \left( \hat{A}_{ij,\phi} - \hat{A}_{ij,\psi} \right) - (A_{ij,\phi} - A_{ij,\psi}) \right] \left[ \left( \hat{A}_{ij,\phi} - \hat{A}_{ij,\psi} \right) + (A_{ij,\phi} - A_{ij,\psi}) \right] \right| \\
 946 \quad & \leq \kappa \left( \left\| \hat{\Sigma}_\phi^{-\lambda} - \Sigma_\phi^{-\lambda} \right\|_{\mathcal{L}^\infty(\mathcal{H}_\phi)} + \left\| \hat{\Sigma}_\psi^{-\lambda} - \Sigma_\psi^{-\lambda} \right\|_{\mathcal{L}^\infty(\mathcal{H}_\psi)} \right) \times \left( \frac{2\kappa}{\lambda} + \frac{2\kappa}{\lambda} \right) \\
 947 \quad & = \frac{4\kappa^2}{\lambda} \left[ \left\| \hat{\Sigma}_\phi^{-\lambda} - \Sigma_\phi^{-\lambda} \right\|_{\mathcal{L}^\infty(\mathcal{H}_\phi)} + \left\| \hat{\Sigma}_\psi^{-\lambda} - \Sigma_\psi^{-\lambda} \right\|_{\mathcal{L}^\infty(\mathcal{H}_\psi)} \right] \\
 948 \quad & \leq \frac{4\kappa^2}{\lambda^3} \left[ \left\| \hat{\Sigma}_\phi - \Sigma_\phi \right\|_{\mathcal{L}^2(\mathcal{H}_\phi)} + \left\| \hat{\Sigma}_\psi - \Sigma_\psi \right\|_{\mathcal{L}^2(\mathcal{H}_\psi)} \right]. \tag{19}
 \end{aligned}$$

949 Let us define  $Z_i^\phi = K_\phi(\cdot, X_i) \otimes_{\mathcal{H}_\phi} K_\phi(\cdot, X_i)$ . Then,  $Z_i^\phi$ 's are i.i.d random variables,  $\mathbb{E}(Z_i^\phi) = \Sigma_\phi$  and  $\hat{\Sigma}_\phi - \Sigma_\phi = \frac{1}{n} \sum_{i=1}^n [Z_i^\phi - \mathbb{E}(Z_i^\phi)]$ . Similarly, let us define  $Z_i^\psi = K_\psi(\cdot, X_i) \otimes_{\mathcal{H}_\psi} K_\psi(\cdot, X_i)$ . Then  $Z_i^\psi$ 's are i.i.d random variables,  $\mathbb{E}(Z_i^\psi) = \Sigma_\psi$  and  $\hat{\Sigma}_\psi - \Sigma_\psi = \frac{1}{n} \sum_{i=1}^n [Z_i^\psi - \mathbb{E}(Z_i^\psi)]$ .

950 Note that,

$$\begin{aligned}
 951 \quad & \left\| Z_i^\phi \right\|_{\mathcal{L}^2(\mathcal{H}_\phi)} = \sqrt{\langle Z_i^\phi, Z_i^\phi \rangle_{\mathcal{L}^2(\mathcal{H}_\phi)}} \\
 952 \quad & = \langle K_\phi(\cdot, X_i), K_\phi(\cdot, X_i) \rangle_{\mathcal{H}_\phi} \\
 953 \quad & = K_\phi(X_i, X_i) \\
 954 \quad & \leq \kappa := B.
 \end{aligned}$$

955 Further,

$$\begin{aligned}
 956 \quad & \mathbb{E} \left\| Z_i^\phi - \mathbb{E}(Z_i^\phi) \right\|_{\mathcal{L}^2(\mathcal{H}_\phi)}^2 = \mathbb{E} \left[ \langle Z_i^\phi, Z_i^\phi \rangle_{\mathcal{L}^2(\mathcal{H}_\phi)} \right] - \langle \Sigma_\phi, \Sigma_\phi \rangle_{\mathcal{L}^2(\mathcal{H}_\phi)} \\
 957 \quad & \leq \mathbb{E} \left[ \langle Z_i^\phi, Z_i^\phi \rangle_{\mathcal{L}^2(\mathcal{H}_\phi)} \right] \\
 958 \quad & = \mathbb{E} \left[ \langle K_\phi(\cdot, X_i), K_\phi(\cdot, X_i) \rangle_{\mathcal{H}_\phi}^2 \right] \\
 959 \quad & = \mathbb{E} [K_\phi(X_i, X_i)^2] \\
 960 \quad & \leq \kappa^2 := \theta^2.
 \end{aligned}$$

990 Similarly, we can show that  $\|Z_i^\psi\|_{\mathcal{L}^2(\mathcal{H}_\psi)} \leq \kappa = B$  and  $\mathbb{E} \|Z_i^\phi - \mathbb{E}(Z_i^\phi)\|_{\mathcal{L}^2(\mathcal{H}_\phi)}^2 \leq \kappa^2 = \theta^2$ .  
 991

992 Note that since  $K(\cdot, \cdot)$  is bounded and continuous,  $\mathcal{H}_\phi$  and  $\mathcal{H}_\psi$  are separable Hilbert spaces. Now, using Bernstein's  
 993 inequality for separable Hilbert spaces (Theorem D.1 in [Sriperumbudur & Sterge \(2022\)](#)), we have that, for any  $0 < \delta < 1$ ,  
 994

$$995 P \left( \|\hat{\Sigma}_\phi - \Sigma_\phi\|_{\mathcal{L}^2(\mathcal{H}_\phi)} \geq \frac{2\kappa \log(\frac{6}{\delta})}{n} + \sqrt{\frac{2\kappa^2 \log(\frac{6}{\delta})}{n}} \right) \leq \frac{\delta}{3}$$

996 and  
 997

$$1000 P \left( \|\hat{\Sigma}_\psi - \Sigma_\psi\|_{\mathcal{L}^2(\mathcal{H}_\psi)} \geq \frac{2\kappa \log(\frac{6}{\delta})}{n} + \sqrt{\frac{2\kappa^2 \log(\frac{6}{\delta})}{n}} \right) \leq \frac{\delta}{3}.$$

1001 Therefore, we have that, for any  $0 < \delta < 1$ ,

$$1002 P \left( \mathbf{A} = \left| \left[ \tilde{d}_{\lambda}^{\text{UKP}}(\phi, \psi) \right]^2 - \left[ \tilde{d}_{\lambda}^{\text{UKP}}(\phi, \psi) \right]^2 \right| \geq \frac{8\kappa^2}{\lambda^3} \left[ \frac{2\kappa \log(\frac{6}{\delta})}{n} + \sqrt{\frac{2\kappa^2 \log(\frac{6}{\delta})}{n}} \right] \right) \leq \frac{2\delta}{3}.$$

1003 We now proceed to bound  $\mathbf{B}$ .  
 1004

1005 Let us define  
 1006

$$1007 b_{ij} := \frac{1}{n^2} \left[ \left\langle \Sigma_\phi^{-\frac{\lambda}{2}} K_\phi(\cdot, X_i), \Sigma_\phi^{-\frac{\lambda}{2}} K_\phi(\cdot, X_j) \right\rangle_{\mathcal{H}_\phi} - \left\langle \Sigma_\psi^{-\frac{\lambda}{2}} K_\psi(\cdot, X_i), \Sigma_\psi^{-\frac{\lambda}{2}} K_\psi(\cdot, X_j) \right\rangle_{\mathcal{H}_\psi} \right]^2 \\ 1008 = \frac{1}{n^2} [A_{ij,\phi} - A_{ij,\psi}]^2.$$

1009 Then, clearly, we have that  $(b_{ij})_{i,j=1, i \neq j}^n$ 's are i.i.d random variables. Similarly,  $(b_{ii})_{i=1}^n$  are i.i.d random variables. Further,  
 1010  $\mathbb{E}(b_{ij}) = \frac{[d_{\lambda,K}^{\text{UKP}}(\phi, \psi)]^2}{n^2}$  if  $i \neq j$  and  $|b_{ij}| \leq \frac{1}{n^2} [|A_{ij,\phi}| + |A_{ij,\psi}|]^2 \leq \frac{4\kappa^2}{\lambda^2 n^2}$  for any  $i, j$ . Therefore,  $|\mathbb{E}(b_{ij})| \leq \mathbb{E}|b_{ij}| \leq \frac{4\kappa^2}{\lambda^2 n^2}$   
 1011 for any  $i, j$  and  $[d_{\lambda,K}^{\text{UKP}}(\phi, \psi)]^2 \leq \frac{4\kappa^2}{\lambda^2}$ .

1012 Now, we have that,  $\mathbb{E} [\tilde{d}_{\lambda}^{\text{UKP}}(\phi, \psi)]^2 = \frac{n(n-1)}{n^2} [d_{\lambda,K}^{\text{UKP}}(\phi, \psi)]^2 + n\mathbb{E}(b_{11})$ . Consequently,  $[d_{\lambda,K}^{\text{UKP}}(\phi, \psi)]^2 -$   
 1013  $\mathbb{E} [\tilde{d}_{\lambda}^{\text{UKP}}(\phi, \psi)]^2 = \frac{1}{n} [d_{\lambda,K}^{\text{UKP}}(\phi, \psi)]^2 - n\mathbb{E}(b_{11})$ . Therefore,  $\left| [d_{\lambda,K}^{\text{UKP}}(\phi, \psi)]^2 - \mathbb{E} [\tilde{d}_{\lambda}^{\text{UKP}}(\phi, \psi)]^2 \right| \leq \frac{8\kappa^2}{\lambda^2 n}$ .  
 1014

1015 Now, using McDiarmid's inequality, we have that,  
 1016

$$1017 P \left( \left| [d_{\lambda}^{\text{UKP}}(\phi, \psi)]^2 - \mathbb{E} [\tilde{d}_{\lambda}^{\text{UKP}}(\phi, \psi)]^2 \right| \geq \frac{4\kappa^2}{\lambda^2} \sqrt{\frac{2 \log(\frac{6}{\delta})}{n}} \right) \leq \frac{\delta}{3}.$$

1018 Therefore, we have that,  
 1019

$$1020 P \left( \mathbf{B} \geq \frac{\kappa^2}{\lambda^2} \left[ \frac{8}{n} + 4\sqrt{\frac{2 \log(\frac{6}{\delta})}{n}} \right] \right) \leq \frac{\delta}{3}.$$

1021 Finally, we have that,  
 1022

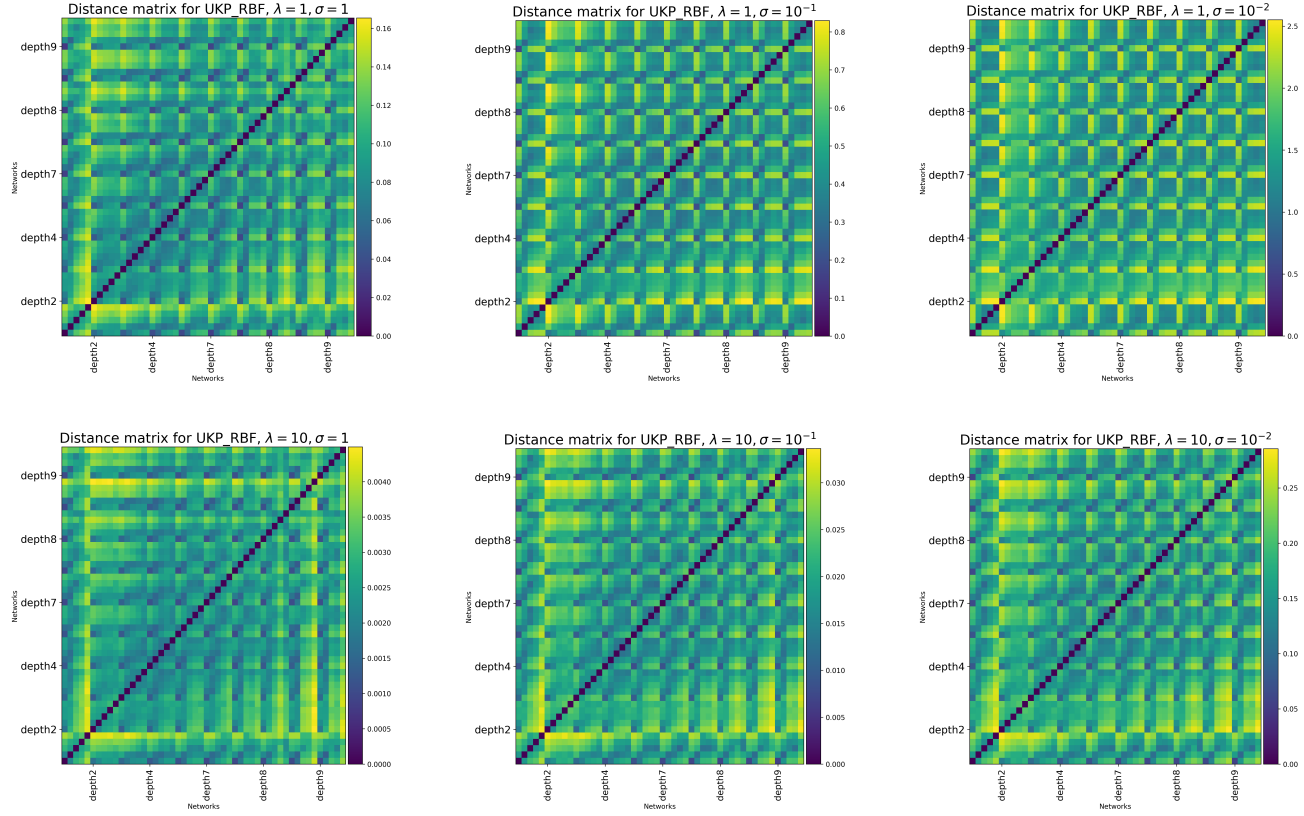
$$1023 P \left( \mathbf{A} + \mathbf{B} \leq \frac{8\kappa^3}{\lambda^3} \left[ \frac{2 \log(\frac{6}{\delta})}{n} + \sqrt{\frac{2 \log(\frac{6}{\delta})}{n}} \right] + \frac{4\kappa^2}{\lambda^2} \left[ \frac{2}{n} + \sqrt{\frac{2 \log(\frac{6}{\delta})}{n}} \right] \right) \geq 1 - \delta,$$

1024 which completes the proof.  $\square$   
 1025

## 1045 A.2. Additional Experiments

### 1046 A.2.1. MNIST EXPERIMENTS

1048 **Training details** We have already described the architectures of the 50 ReLU networks we trained for experiments using  
 1049 the MNIST dataset in Section 5.1. We used the uniform Kaiming initialization (He et al., 2015) for initializing the network  
 1050 weights for every network with a specific width and depth, while the biases are set to zero at initialization. We used a single  
 1051 A100 GPU on the Google Colab platform. We chose to use the Adam optimizer with a learning rate of  $10^{-4}$  and a batch  
 1052 size of 100 to train the 50 ReLU networks. We follow a training scheme similar to that used in Boix-Adsera et al. (2022).  
 1053



1055 **Figure 3:** Heatmaps representing UKP distance between pairs of fully-connected ReLU networks of different depths and  
 1056 widths. We choose the kernel for the UKP distance to be the Gaussian RBF kernel with bandwidth  $\sigma \in \{1, 10^{-1}, 10^{-2}\}$   
 1057 along with the regularization parameter  $\lambda \in \{1, 10\}$ . Along the rows and columns of each of the heatmaps, the ReLU  
 1058 networks are first arranged in order of increasing depth, and then in order of increasing width inside each specific depth  
 1059 level. Darker colors indicate smaller value of UKP distance according to the scale attached to each heatmap.  
 1060

1061 **Clustering of representations based on UKP aligns with architectural characteristics of networks** We observe in  
 1062 Fig. 3 that a repeating block structure emerges in each heatmap, with each block corresponding to networks with the same  
 1063 depth. Within each block, i.e., same depth, the pairwise similarities between networks with different widths are higher if  
 1064 the difference of widths of the pair of networks is small, and the similarities are lower otherwise. Further, it seems that  
 1065 the relative difference between networks with different depths is amplified (in terms of the UKP distance) if the depths  
 1066 of the networks are larger. For e.g. the contrast between a width 500 and width 600 network is higher when the depth  
 1067 is 9 for both networks, compared to the scenario where both networks have depth 2. We also perform an agglomerative  
 1068 (bottom-up) hierarchical clustering of the representations based on the pairwise UKP distances and obtain the corresponding  
 1069 dendograms as shown in Fig. 4. The dendograms also exhibit separation between deeper networks (depths 7,8 and 9) and  
 1070 shallower networks (depths 2,4 and 6) over a range of  $(\lambda, \sigma)$  choices for the UKP distance with Gaussian RBF kernel. This  
 1071 indicates that the UKP distance is able to capture the relevant differences in predictive performance that are induced by  
 1072 architectural differences in these networks, over a wide range of values of its tuning parameters.  
 1073

## Uniform Kernel Prober

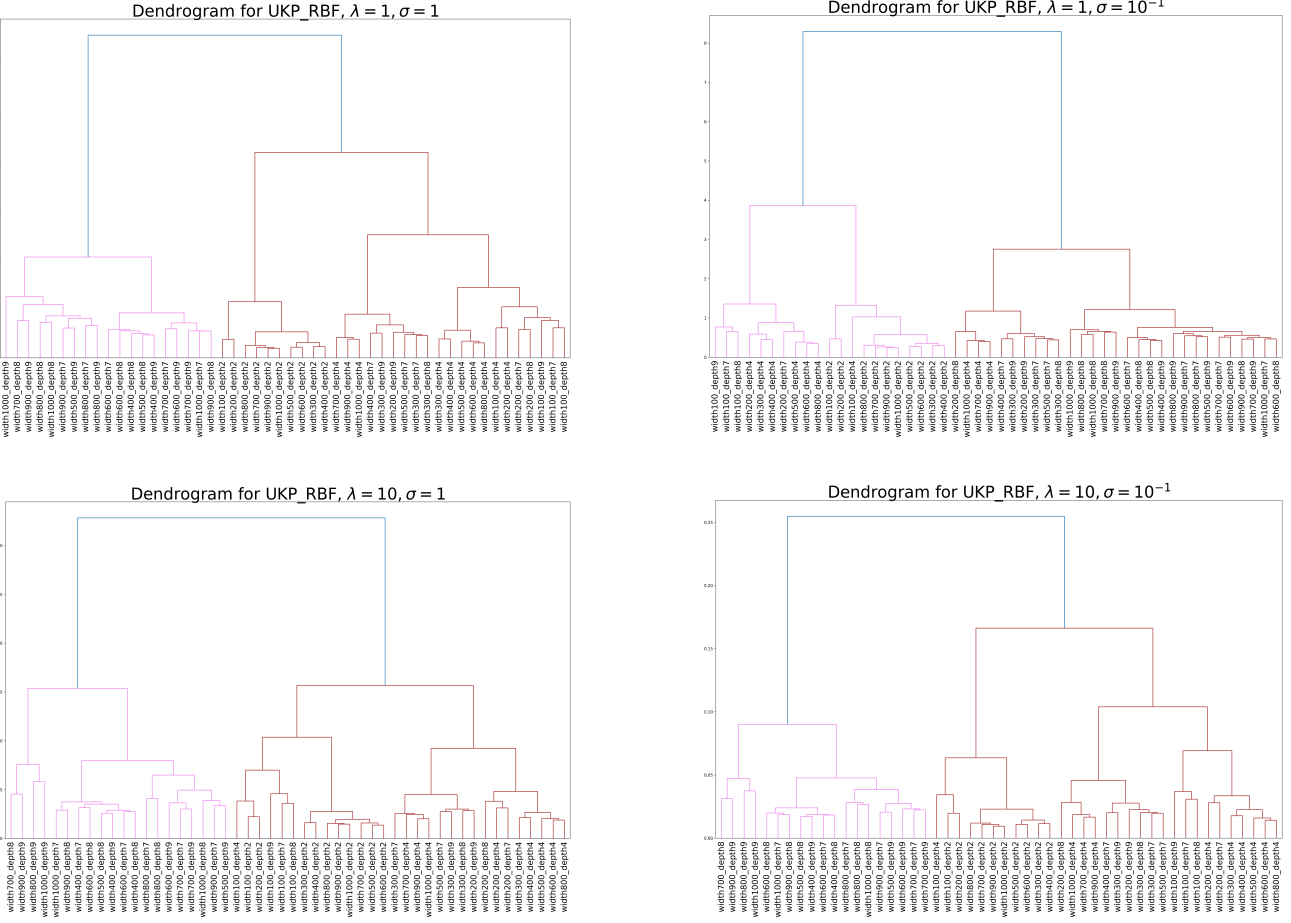


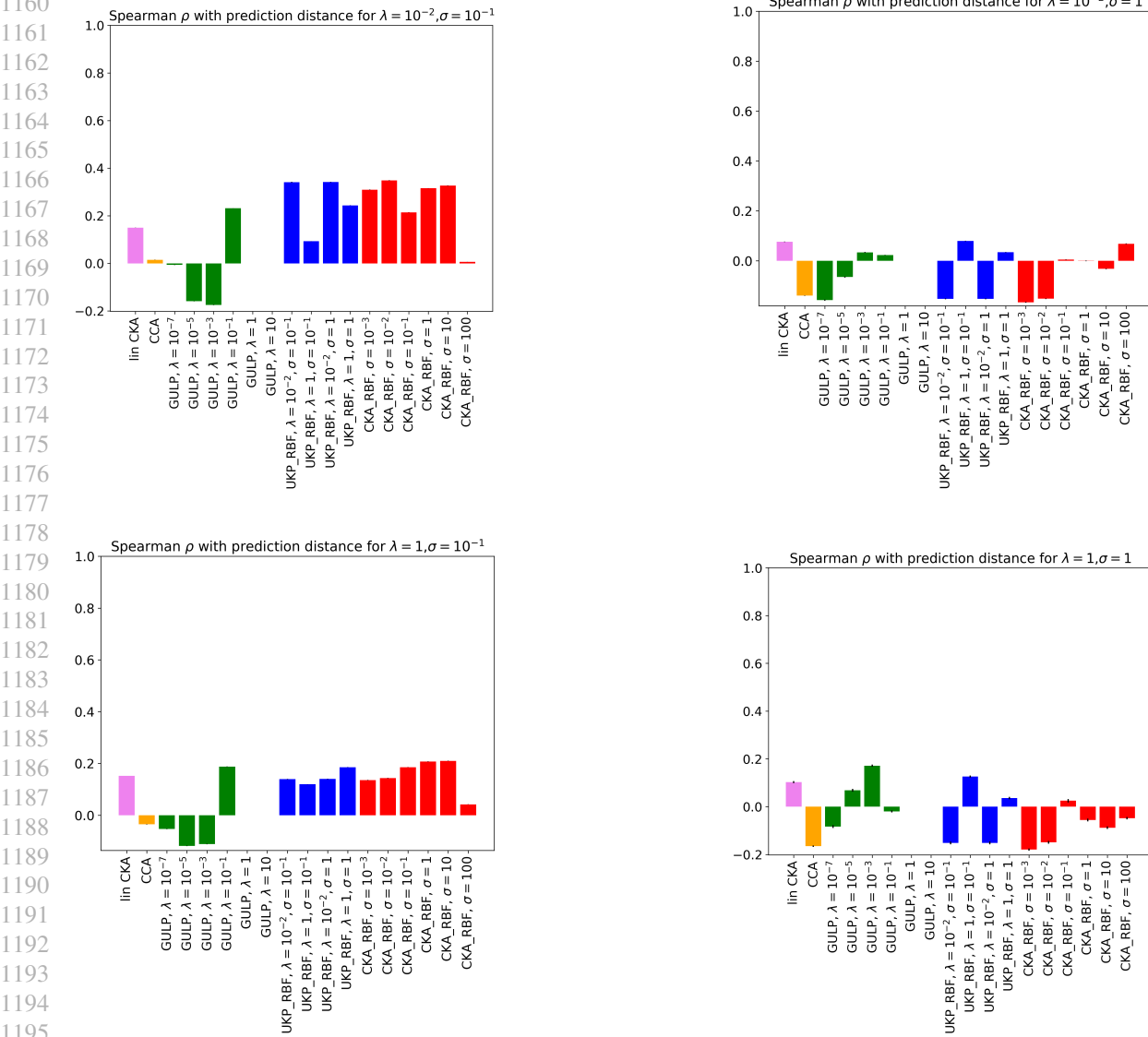
Figure 4: Dendrograms corresponding to agglomerative hierarchical clustering of representations of 50 ReLU networks based on UKP distance

**Generalization ability on kernel ridge regression tasks** We consider the same setup as discussed in Section 5.1. Supplementing our choices of  $\lambda = 10^{-2}$  and  $\sigma = 10^{-1}$  corresponding to synthetic kernel ridge regression tasks with Gaussian RBF kernel, we now consider  $\lambda \in \{10^{-2}, 1\}$  and  $\sigma \in \{10^{-1}, 1\}$ . In Fig. 5, we plot the Spearman’s  $\rho$  rank correlation coefficient between the  $err_{\phi,\psi}$ ’s as defined in Section 5.1 and the pairwise distances between the representations using the following distances - CCA, linear CKA, nonlinear CKA with Gaussian RBF kernel, GULP and UKP with Gaussian RBF kernel.

When  $(\lambda = 10^{-2}, \sigma = 10^{-1})$  and  $(\lambda = 1, \sigma = 10^{-1})$ , we observe from Fig. 5 that the pairwise UKP distance is positively correlated to a moderate extent with the collection of  $err_{\phi,\psi}$ ’s, as evident from the large positive values of the blue bars. In contrast, GULP distances show inconsistent behavior across different levels of regularization, while CCA and linear CKA distances show a much lower positive correlation with generalization performance (with CCA even showing negative correlation when  $(\lambda = 1, \sigma = 10^{-1})$ ). For the remaining choices, none of the distance measures show any consistent behavior, which indicates that an increase in the number of samples used to approximate the model representations may improve the performance of these distance measures.

Unsurprisingly, as a consequence of the relationship between CKA and UKP, as discussed in Section 4.1, the performance of the CKA distance, when using the Gaussian RBF kernel (with the corresponding bars shown in red), is comparable to that of UKP with the same choice of kernel. This similarity in the information conveyed by these two measures can be empirically observed through their scatterplots and the Pearson product-moment correlation coefficient under various choices of tuning parameters. As shown in Fig. 6, the nearly linear positive relationship between UKP and CKA distances, when both are used with a Gaussian RBF kernel, along with the high positive correlation coefficient, suggests that either

1155 measure could be effectively used in practice for comparing representations. However, the UKP distance may be preferred  
 1156 over the CKA distance due to its pseudometric properties, particularly the triangle inequality, which proves to be especially  
 1157 useful. In contrast, CKA, being a measure akin to a normalized inner product bounded between 0 and 1, does not satisfy the  
 1158 properties of a pseudometric and may lead to misleading intuitions when comparing different representations.  
 1159



1166 Figure 5: Spearman's  $\rho$  rank correlation coefficient between generalization of kernel ridge regression-based predictors with  
 1167 various distance measures between representations. We report the average correlation across 10 random synthetic kernel  
 1168 ridge regression tasks. Results are similar for 30 trials. Error bars are negligibly small and hence not visible.  
 1169

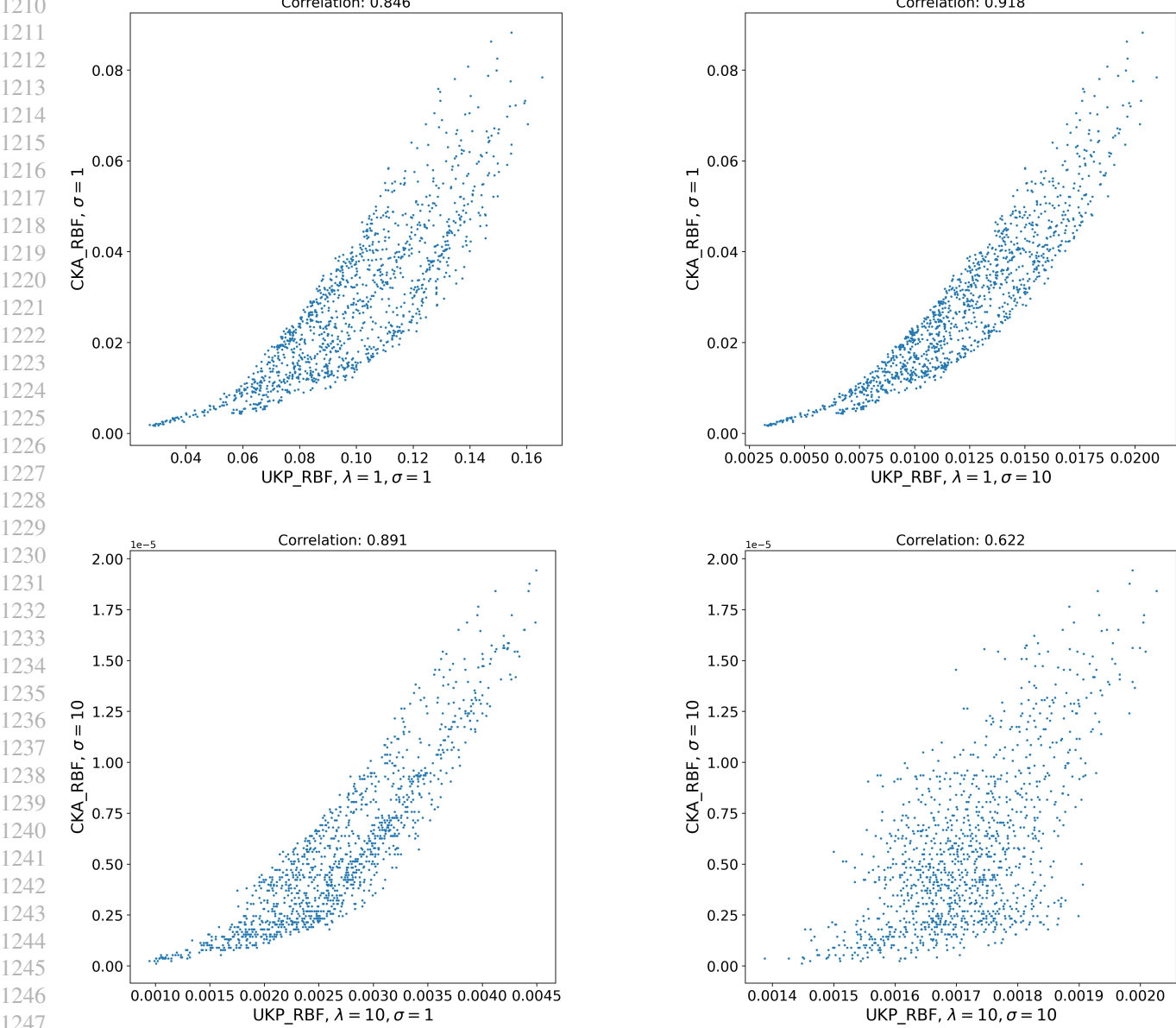


Figure 6: Correlation plots between UKP and CKA measures with Gaussian RBF kernel between  $\binom{50}{2}$  pairs of ReLU networks trained on MNIST data. Plot titles display the Pearson product-moment correlation coefficient between the distance measures on the two axes.

#### A.2.2. IMAGENET EXPERIMENTS

**Architectures used and data description** In our experiments, we utilized 35 pretrained models known for achieving state-of-the-art (SOTA) performance in the ImageNet Object Localization Challenge on Kaggle (Howard et al., 2018), available from PyTorch (2024). These models are categorized based on their architectural types as follows:

- **ResNets (17 models):** regnet\_x\_16gf, regnet\_x\_1\_6gf, regnet\_x\_32gf, regnet\_x\_3\_2gf, regnet\_x\_400mf, regnet\_x\_800mf, regnet\_x\_8gf, regnet\_y\_16gf, regnet\_y\_1\_6gf, regnet\_y\_32gf, regnet\_y\_3\_2gf, regnet\_y\_400mf, regnet\_y\_800mf, regnet\_y\_8gf, resnet18, resnext50\_32x4d, wide\_resnet50\_2
- **EfficientNets (8 models):** efficientnet\_b0, efficientnet\_b1, efficientnet\_b2, efficientnet\_b3, efficientnet\_b4, efficientnet\_b5, efficientnet\_b6, efficientnet\_b7

- **MobileNets (3 models):** mobilenet\_v2, mobilenet\_v3\_large, mobilenet\_v3\_small
- **ConvNeXts (2 models):** convnext\_small, convnext\_tiny
- **Other Architectures (5 models):** alexnet, googlenet, inception, mnasnet, vgg16 .

The penultimate layer dimensions for these networks, corresponding to the representation sizes, vary from 400 to 4096 depending on the architecture. Each model processes input data as 3-channel RGB images, with each channel having dimensions of  $224 \times 224$  pixels. To approximate the model representations learned by these models using finite-dimensional representations, we used 3000 images from the validation set of the ImageNet dataset. These images were normalized with a mean of (0.485, 0.456, 0.406) and a standard deviation of (0.229, 0.224, 0.225) for each RGB channel. Our choice of models and input preprocessing parameters is similar to those used in Boix-Adsera et al. (2022).

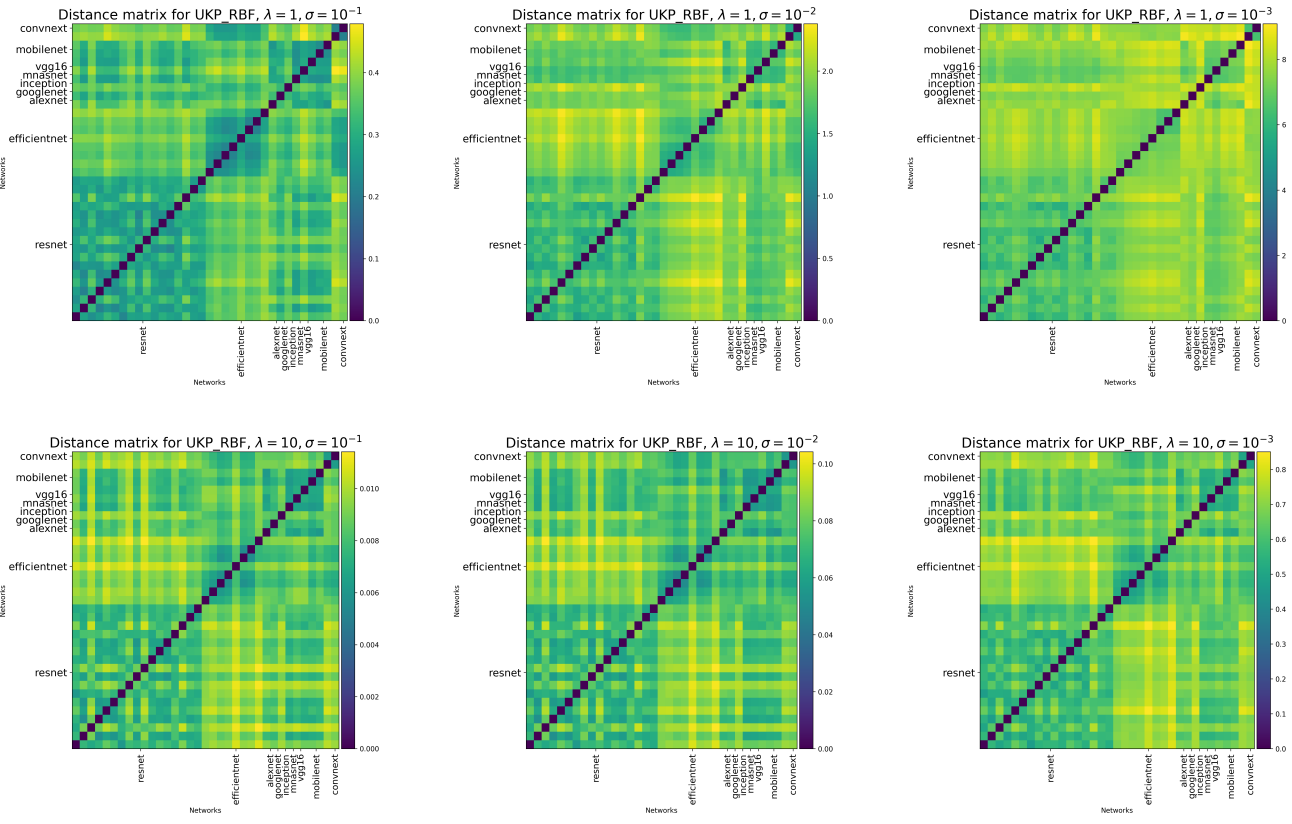


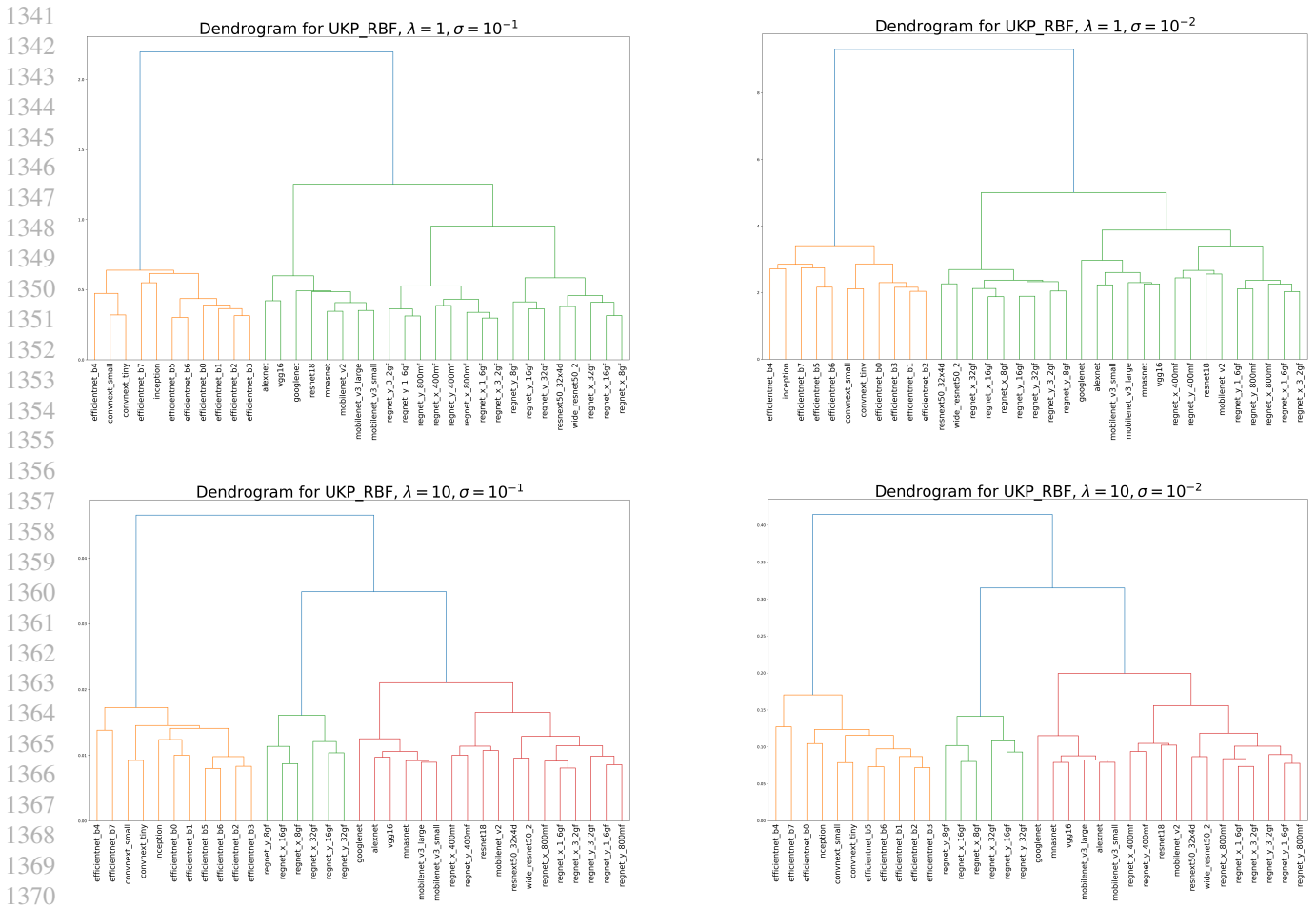
Figure 7: Heatmaps representing UKP distance between pairs of networks of different architecture, pretrained on ImageNet data. We choose the kernel for the UKP distance to be the Gaussian RBF kernel with bandwidth  $\sigma \in \{10^{-1}, 10^{-2}, 10^{-3}\}$  along with the regularization parameter  $\lambda \in \{1, 10\}$ . Along the rows and columns of each of the heatmaps, the networks are arranged in the following order from left to right and top to bottom - ResNets, EfficientNets, Other Architectures, MobileNets and ConvNeXts. Darker colors indicate smaller value of UKP distance according to the scale attached to each heatmap.

**Clustering of representations based on UKP aligns with architectural characteristics of networks** We are interested in observing whether the UKP pseudometric is capable of capturing intrinsic differences in predictive performances of different representations. Such intrinsic differences are often the result of the different inductive biases we encode into networks through the choice of architectures, among other factors.

We first discuss the main architectural similarities and differences between ResNet, RegNet, EfficientNet, MobileNet, alexnet, googlenet, inception, mnasnet, and vgg16, which are controlled by how they address depth, efficiency, and feature extraction. Alexnet and vgg16 are older architectures that use standard convolutional layers arranged in sequential blocks,

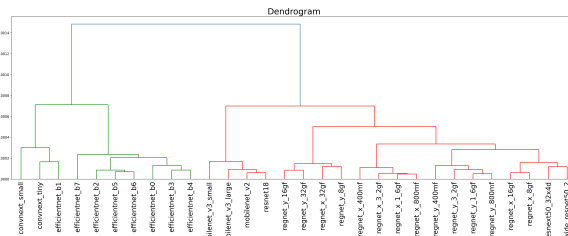
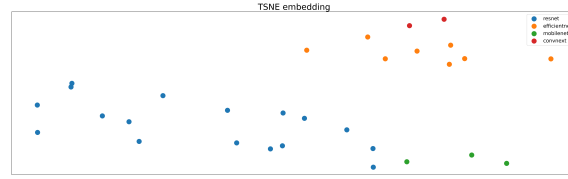
1320 with vgg16 deepening the network significantly compared to alexnet. Googlenet introduced Inception modules, which  
 1321 combine multiple convolution filters of different sizes to capture multi-scale features, making it more efficient than alexNet  
 1322 and vgg16. Different Inception architectures have been built using the Inception module of Googlenet. ResNet brought  
 1323 the innovation of residual connections (skip connections) to address the vanishing gradient problem, enabling very deep  
 1324 networks, while RegNet refined this concept by creating more regular, scalable structures without explicit skip connections.  
 1325 EfficientNet and mnasnet focus on balanced scaling (depth, width, resolution) and use of MBConv blocks for efficiency,  
 1326 with EfficientNet employing a compound scaling formula. MobileNet, like mnasnet, emphasizes depthwise separable  
 1327 convolutions for lightweight, efficient models suitable for mobile devices. In terms of architectural similarities, resNet and  
 1328 regNet share a focus on structured deep architectures, while EfficientNet and MobileNet share efficiency-driven designs for  
 1329 varied hardware constraints. Alexnet, vgg16, and googlenet represent early convolutional architectures, with googlenet's  
 1330 Inception modules providing a bridge to more modern designs. In contrast, vgg16 and ResNet are quite different, with  
 1331 vgg16 being sequential and deep, and ResNet leveraging residual connections.

1332 We observe in Fig. 7 that a block structure emerges in the heatmaps across different choices of the tuning parameters for  
 1333 the UKP distance, especially corresponding to the 4 major groups of architectures ResNets, EfficientNets, MobileNets  
 1334 and ConvNeXts. We also perform an agglomerative (bottom-up) hierarchical clustering of the representations based on  
 1335 the pairwise UKP distances and obtain the corresponding dendograms as shown in Fig. 8. The dendograms exhibit a  
 1336 clear separation between the ResNets/RegNets and the remaining architectures over a range of  $(\lambda, \sigma)$  choices for the UKP  
 1337 distance with Gaussian RBF kernel. This indicates that, for the class of pretrained ImageNet models we consider, the UKP  
 1338 distance captures the relevant differences in predictive performance that are induced by architectural differences in these  
 1339 networks, over a wide range of values of its tuning parameters.

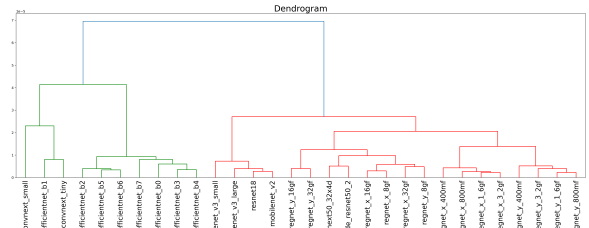
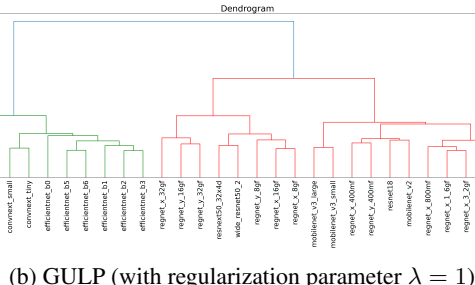
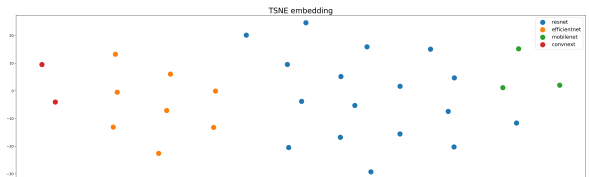
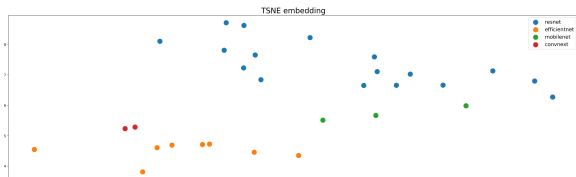


1371 Figure 8: Dendograms corresponding to agglomerative hierarchical clustering of representations of 35 pretrained ImageNet  
 1372 networks based on UKP distance

To illustrate that the performance of the UKP pseudometric is reasonably robust to the choice of the regularization parameter  $\lambda$  and kernel parameters (such as bandwidth parameter  $\sigma$  for the Gaussian RBF kernel), we have compared the performance of UKP's performance with other popular baseline measures such as GULP and CKA. As observed from Fig. 9, the separation between the different classes of networks is more pronounced in the case of UKP than GULP. Additionally, the clustering behaviour within the primary classes of networks is much weaker for the CKA compared to the UKP and GULP measures, and the separation between the different classes is not clear in the case of CKA.



(a) UKP (with RBF kernel, regularization parameter  $\lambda = 1$  and kernel bandwidth  $\sigma = 10$ )



(b) GULP (with regularization parameter  $\lambda = 1$ )

(c) CKA (with RBF kernel and kernel bandwidth  $\sigma = 10$ )

Figure 9: t-SNE embeddings and dendrograms corresponding to agglomerative hierarchical clustering of representations of 35 pretrained ImageNet networks based on UKP (with Gaussian RBF kernel, regularization parameter  $\lambda = 1$  and kernel bandwidth  $\sigma = 10$ ), GULP (with regularization parameter  $\lambda = 1$ ) and CKA (with Gaussian RBF kernel and kernel bandwidth  $\sigma = 10$  distance)

**Relationship between UKP and CKA measures** The MNIST experiments, along with the theoretical analysis in section 4.1, reveal a similarity between the information conveyed by the UKP and CKA measures when both use the same kernel. This similarity is also empirically confirmed in the ImageNet experiments, as demonstrated by their scatterplots and the Pearson correlation coefficient across different tuning parameters. As illustrated in Fig. 10, there is an almost linear positive relationship between UKP and CKA distances when both utilize a Gaussian RBF kernel. The strong positive correlation suggests that either measure could be effectively used for comparing representations. However, as previously discussed in Section 4.1, UKP may be preferred over CKA due to its pseudometric properties, particularly the triangle inequality, which

is especially advantageous. In contrast, CKA, being a measure similar to a normalized inner product bounded between 0 and 1, does not satisfy pseudometric properties and may lead to misleading interpretations when comparing different representations.

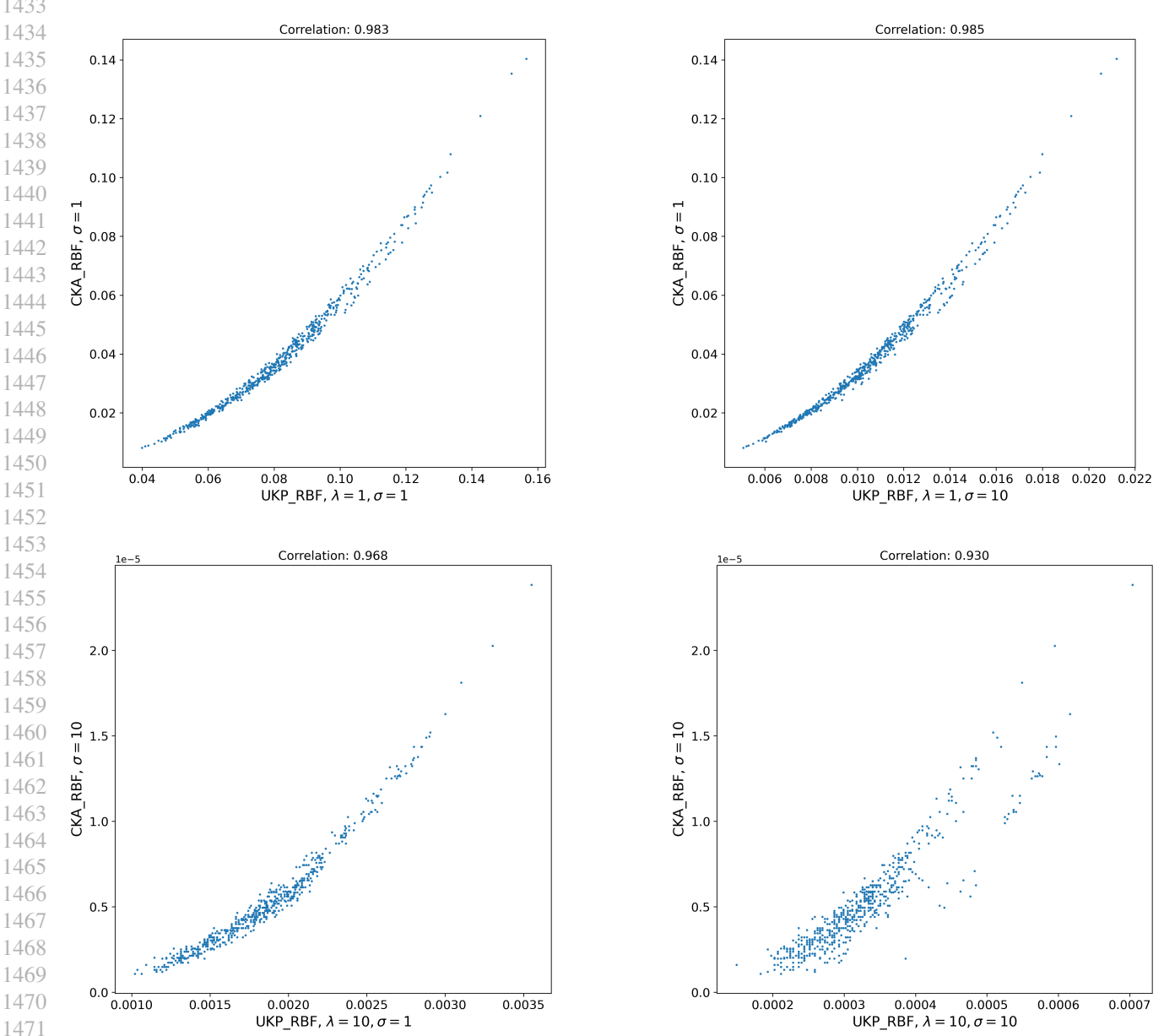


Figure 10: Correlation plots between UKP and CKA measures with Gaussian RBF kernel between  $\binom{35}{2}$  pairs of networks with different architectures trained on ImageNet data. Plot titles display the Pearson product-moment correlation coefficient between the distance measures on the two axes.

**Choice of kernel function** The choice of kernel function for the UKP pseudometric should be guided by the inductive bias most relevant to the tasks for which the representations or features of interest will be used. For instance, consider an image classification task where the model's predictions should remain unaffected by image rotations. In this case, we can incorporate this inductive bias into the UKP pseudometric by selecting a rotationally invariant kernel, such as the Gaussian RBF kernel, as the kernel function for UKP. This approach is particularly useful for comparing the generalization performance of two representations: one obtained through a training or optimization procedure that explicitly enforces rotational invariance and another trained without such constraints.

1485 Furthermore, even when the true inductive bias is unknown, probing the nature of representations encoded by different  
1486 models can still provide valuable insights. In this context, the terms “well-specified” and “misspecified” kernels refer,  
1487 respectively, to choices of kernels for the UKP pseudometric that either capture or fail to capture the required inductive  
1488 bias for a specific class of downstream tasks utilizing the representations or features of interest. Each kernel choice can be  
1489 viewed as a selection of particular characteristics of the representations that we aim to investigate.

1490 If we have a set of characteristics in mind that we wish to probe, we should select a corresponding set of kernels whose  
1491 feature maps encode some or all of those characteristics and then analyze the conclusions drawn from using each kernel as  
1492 the kernel function for the UKP pseudometric. When the kernels are “well-specified”, clustering representations based on  
1493 UKP values can help identify useful pairs of representations for specific downstream tasks. In contrast, when the kernels  
1494 are “misspecified”, the UKP values may still cluster representations with characteristics aligned with the feature maps  
1495 of the “misspecified” kernels. However, in such cases, the clustering will not be informative for studying generalization  
1496 performance on downstream tasks. Nonetheless, even with “misspecified kernels”, the UKP pseudometric can still provide  
1497 insights into the characteristics of the representations, though its values will not reliably indicate generalization performance.  
1498

1499 Cross-validation or selecting an “optimal” value for the kernel parameters is not necessary in the context of this paper,  
1500 as our focus is on an exploratory comparison of the inductive biases encoded by different representations. For example,  
1501 consider a scenario where we hypothesize that rotational invariance is the key inductive bias required for good generalization  
1502 performance, as in image classification tasks. In this case, the Gaussian RBF kernel is a natural choice. Since the Gaussian  
1503 RBF kernel remains rotationally invariant for any value of its bandwidth parameter—which controls the “scale” at which  
1504 the kernel perceives the representations—the UKP pseudometric should, in principle, capture the extent to which different  
1505 representations encode rotational invariance, regardless of the specific choice of bandwidth.

1506 Of course, no experimental setup is ever exhaustive. In our study, we focus on datasets from the image domain (MNIST and  
1507 ImageNet) to illustrate one of the simplest and most fundamental invariances—rotational invariance—which is relevant to  
1508 most image-related tasks. This consideration motivated our choice of the Gaussian RBF kernel as the kernel function for the  
1509 UKP pseudometric in our experiments.  
1510

1511 **Code implementation** The Python code for running all the experiments in this paper is available in the following  
1512 Anonymous GitHub repository: <https://github.com/ICMLsubmision8890/Uniform-Kernel-Prober>.  
1513 The code for comparing our proposed UKP pseudometric to other distance measures has been adapted from <https://github.com/sgstepanants/GULP>.  
1514  
1515

1516  
1517  
1518  
1519  
1520  
1521  
1522  
1523  
1524  
1525  
1526  
1527  
1528  
1529  
1530  
1531  
1532  
1533  
1534  
1535  
1536  
1537  
1538  
1539